



Diazotrophy in the Indian Ocean: Current understanding and future perspectives

Subhadeep Chowdhury, Eric Raes, Cora Hörstmann, Ayaz Ahmed, Céline Ridame, Nicolas Metzl, P Bhavya, Takuya Sato, Takuhei Shiozaki, Sophie Bonnet, et al.

► To cite this version:

Subhadeep Chowdhury, Eric Raes, Cora Hörstmann, Ayaz Ahmed, Céline Ridame, et al.. Diazotrophy in the Indian Ocean: Current understanding and future perspectives. *Limnology and Oceanography Letters*, 2023, 8 (5), pp.707-722. 10.1002/lol2.10343 . hal-04239722

HAL Id: hal-04239722

<https://hal.science/hal-04239722>

Submitted on 13 Oct 2023







HAL is a multi-disciplinary open access archive for the deposit and dissemination of scientific research documents, whether they are published or not. The documents may come from teaching and research institutions in France or abroad, or from public or private research centers.

L'archive ouverte pluridisciplinaire **HAL**, est destinée au dépôt et à la diffusion de documents scientifiques de niveau recherche, publiés ou non, émanant des établissements d'enseignement et de recherche français ou étrangers, des laboratoires publics ou privés.



Distributed under a Creative Commons Attribution 4.0 International License

CURRENT EVIDENCE

Diazotrophy in the Indian Ocean: Current understanding and future perspectives**Subhadeep Chowdhury** ^{1,2}, **Eric Raes**³, **Cora Hörstmann**^{1,2}, **Ayaz Ahmed**⁴, **Céline Ridame**⁵, **Nicolas Metzl**⁵, **P S Bhavya**⁶, **Takuya Sato** ⁷, **Takuhei Shiozaki** ⁸, **Sophie Bonnet**¹, **Carolyn R. Löscher** ⁹, **Arvind Singh** ¹⁰, **Mar Benavides** ^{1,2*}¹Aix Marseille Univ, Université de Toulon, CNRS, IRD, MIO UM 110, Marseille, France; ²Turing Center for Living Systems, Aix-Marseille University, Marseille, France; ³Flourishing Oceans, Minderoo Foundation, Nedlands, Western Australia, Australia; ⁴Kuwait Institute for Scientific Research, Salmiya, Kuwait; ⁵Laboratoire LOCEAN/IPSL, Sorbonne Université-CNRS-IRD-MNHN, Paris, France; ⁶Department of Biological Oceanography, Leibniz Institute for Baltic Sea Research, Warnemuende, Rostock, Germany; ⁷Graduate School of Agricultural and Life Sciences, The University of Tokyo, Bunkyo-ku, Tokyo, Japan; ⁸Atmosphere and Ocean Research Institute, The University of Tokyo, Chiba, Japan; ⁹Nordcee, Department of Biology, University of Southern Denmark, Odense, Denmark; ¹⁰Physical Research Laboratory, Ahmedabad, India**Scientific Significance Statement**

Dinitrogen (N₂) fixation provides the largest source of reactive nitrogen in the ocean. The Indian Ocean (IO) accounts for ~1% of the N₂ fixation data available, although it covers 22% of the global ocean surface. Compiling the currently available N₂ fixation data from the IO, we conclude that its magnitude is within the ranges obtained in previous modeling efforts. However, we find that certain sub-basin measurements such as those of the Bay of Bengal, Arabian Sea, and the Eastern Indian Ocean, are particularly variable, pleading for more a comprehensive spatiotemporal sampling in future studies. Finally, we propose future research directions for a better understanding of the contribution of the IO to nitrogen inputs in the global ocean.

Abstract

Dinitrogen (N₂) fixation provides the major source of reactive nitrogen in the open ocean, sustaining biological productivity. The Indian Ocean (IO) covers 22% of the ocean surface, while it only represents 1% of the global diazotroph database. Hence, constraining the sources of nitrogen in the IO is crucial. Here, we compile three decades of N₂ fixation and diazotroph DNA data in the IO. Our analysis reveals basin-scale yearly rates between

*Correspondence: mar.benavides@ird.fr**Associate editor:** Mary Rose Gradoville**Author Contribution Statement:** SC compiled data provided by ER, CH, AA, CR, NM, PSB, TS, TS, CRL, and AS. SC performed statistical analyses, sequence analyses, and plots and led the writing of the review with MB and SB. CH assisted with statistical analyses and illustrations. All authors commented on the text before submission.**Data Availability Statement:** All the N₂ fixation data used in this study are available in Zenodo <https://zenodo.org/record/7870536>. The *nifH* Sanger and amplicon sequences were retrieved from ENA, DDBJ, and NCBI with reference numbers provided in the supporting information (compiled in Appendix S2). The code used for making the figures presented in this study are available from <https://github.com/OceanBridges/Indian-Ocean-review-figures/tree/main>.

Additional Supporting Information may be found in the online version of this article.

This is an open access article under the terms of the [Creative Commons Attribution](https://creativecommons.org/licenses/by/4.0/) License, which permits use, distribution and reproduction in any medium, provided the original work is properly cited.

~ 7 and 13 Tg N yr⁻¹. These rates are in the range of previous modeling-based estimates but may represent a lower bound estimate due to the lack of data in this basin. Diazotroph variability among sub-basins may suggest endemism but needs to be taken with caution due to biased sampling toward certain seasons and uneven spatial coverage. We provide recommendations for a more accurate representation of the IO in the global nitrogen budget and our knowledge of diazotroph biogeography.

A historical perspective of oceanographic research in the Indian Ocean

For more than a century, our knowledge of the Indian Ocean (IO) has been lagging that of other basins in oceanographic research (Hood et al. 2015). The first scientific voyage covering the IO was the Challenger Expedition (1872–1876), which investigated a region between Cape Town and Melbourne to study ocean currents, marine life and chemistry (Branagan 1972). The John Murray expedition (1933–1934), the first expedition solely focusing on the IO, found an acute oxygen deficiency signal in the mesopelagic layer, particularly in the Arabian Sea (AS) (Sewell 1934). The second Expedition (Danish Expedition Galathea, 1950–1952) studied the deep ocean fauna of eastern IO (Marshall 1960). During the International Geophysical Year (1957–1958), several countries including Australia, France, Japan, New Zealand, and the former Soviet Union conducted oceanographic research campaigns in the southern IO. The Scientific Committee on Oceanic Research launched the International Indian Ocean Expedition (IIOE; 1960–1965), representing the first basin-wide survey of the IO. This first IIOE provided capacity building and substantial progress in our understanding of ocean processes in this basin (Wyrki et al. 1971; Hood et al. 2015).

During the 1970s, the Geochemical Ocean Sections Study program investigated biogeochemical and hydrographic parameters in the IO (Weiss 1983). In the following years, the Indian Ocean Experiment (1979) studied the impact of the southwest monsoon (SWM) on the Somali Current on biological and chemical parameter distributions (Swallow 1980, 1984). There were several scientific initiatives in the following years, including the Netherlands Indian Ocean Program (1992–1993) and the World Ocean Circulation Experiment (1988–1998) (Smith 2005; Parambil 2015). The Second International Indian Ocean Expedition (IIOE-2; 2015–2025) was born from the acknowledged need to improve our understanding of oceanic, geological, and atmospheric processes in the IO, as well as their interactions with biogeochemical cycles, ecosystems, and their effect on the regional and global climate (Hood et al. 2015). Despite these efforts, even today the IO remains one of the most under-sampled basins in the world's oceans, receiving a comparatively low number of research projects and large expeditions (Hood et al. 2015).

The interest in nitrogen cycling in the IO started with the 1933–1934 John Murray expedition to the AS, where an acute oxygen deficiency signal was detected in the mesopelagic layer (oxygen concentrations $< 0.1 \text{ mL L}^{-1}$) (Sewell 1934).

Marine microbes use oxygen as an electron acceptor to remineralize organic matter (Carlson et al. 2007). In oxygen deficient zones, fixed nitrogen is removed through denitrification and anammox, which convert nitrate and ammonium into N_2 (Zehr and Ward 2002). Over the years, research on these processes has shown that the AS accounts for half of the global mesopelagic reactive nitrogen loss (Naqvi 1987; Codispoti 2007; Ward et al. 2009; Jayakumar et al. 2012) and represents the second-largest oxygen minimum zone (OMZ) of the global ocean (Bertagnolli and Stewart 2018). At the global scale, the reactive nitrogen deficit created by denitrification and anammox can be alleviated by biological N_2 fixation (Gruber 2008), which is supported by sedimentary $\delta^{15}N$ records pointing toward a stable fixed nitrogen inventory in the Holocene (Brandes and Devol 2002).

N₂ fixation is carried out by diazotrophs: prokaryotes including filamentous and unicellular cyanobacteria, and non-cyanobacterial diazotrophs (NCDs) that may comprise a diverse suite of metabolisms including chemoorganoheterotrophy and chemolithoautotrophy, among others (Turk-Kubo et al. 2022). Due to the high energy demand of this process, N₂ fixation is usually inhibited in the presence of more readily available reactive nitrogen compounds such as ammonium and nitrate (Zehr and Capone 2020). Diazotrophs use the nitrogenase enzyme complex to reduce N₂ to ammonium, an enzyme irreversibly inhibited by oxygen (Postgate 1982). Due to the destructive effect of oxygen on nitrogenase, OMZs have been suggested as potential niches for N₂ fixation in the ocean (Deutsch et al. 2007), including the AS (Dugdale et al. 1964; Devassy et al. 1978; Naqvi 1987; Capone et al. 1998). However, recurring empirical N₂ fixation measurements in the Eastern Tropical South Pacific OMZ have reported low or undetectable rates (Fernandez et al. 2011; Loescher et al. 2014; Jayakumar et al. 2017), with a few exceptions (Dekaezemacker et al. 2013; Fernandez et al. 2015). Discrepancies between relatively high vs. undetectable N₂ fixation rates in OMZ regions are likely explained by methodological biases in stable isotope tracer methods (Selden et al. 2021). The low N₂ fixation activity in the Eastern Tropical South Pacific OMZ is thought to be due to a deficit in iron availability (Knapp et al. 2016; Bonnet et al. 2017), which differs from the AS where eolian iron inputs are recurrent, enhancing diazotrophy (Dugdale et al. 1964; Devassy et al. 1978; Naqvi 1987; Capone et al. 1998).

Between 1958 and 2019, warming in the upper 2000 m of the IO has accounted for $\sim 9\%$ of the global ocean heat

increase, with accelerated warming observed since the late 1990s (Cheng et al. 2022). Future climate predictions suggest that the IO will continue to warm up, enhancing water column stratification and weakening nutrient input to the surface (Roxy et al. 2016). The inhibition of vertical nutrient supply along with sustained aeolian iron supply in the northern IO (Wiggert and Murtugudde 2007) may enhance the role of diazotrophs as the main reactive nitrogen source in the future. The future of diazotrophy to the south (i.e., Equatorial Indian Ocean [EqIO] and the Southern Indian Ocean [SIO]) where aeolian iron inputs are much lower (McGowan and Clark 2008; Grand et al. 2015), is more uncertain.

The IO represents only ~ 1% of the N_2 fixation data compiled in the global diazotrophy database (Luo et al. 2012; Tang et al. 2019a), although it covers 22% of the ocean surface. Such low coverage hampers our understanding of the role of diazotrophs in the contemporary ocean and future predictability in the frame of climate change. Here we compile N_2 fixation rates and diazotroph DNA sequence data gathered in the IO over the past three decades to summarize our current knowledge and identify the main gaps to be filled in future research programs.

N_2 fixation activity in the IO

The IO can be divided into six sub-basins (Box 1; Fig. 1): the AS and the Bay of Bengal (BoB) located in the west and east of the Indian subcontinent, respectively; the EqIO located between 40–100°E and 10°S–10°N (Thandlam et al. 2020); the Indian Ocean subtropical gyre (IOSG) spanning roughly from ~ 40–100°E and 10–35°S and (Baer et al. 2019); the Eastern Indian Ocean (EIO) spanning from ~ 10–40°S and 100–120°E, and the SIO spanning from ~ 40°S until the circumpolar current (Fig. 1). The IO is subject to strong monsoon wind regimes that reverse seasonally (Hood et al. 2017), imprinting strong geographical and seasonal meteorological variability in the IO and creating unique oceanic circulation and biogeochemical patterns in each of its sub-basins (Schott and McCreary 2001; Hood et al. 2009, 2017; Schott et al. 2009;

Phillips et al. 2021; Vinayachandran et al. 2021). The SWM blows to the northeast in boreal summer (June–September), whereas the northeast monsoon (NEM) blows in the opposite direction in boreal winter (November–February). This reversing atmospheric circulation is mirrored by ocean currents, inducing localized coastal upwelling and nutrient enrichment (Hood et al. 2017). In the AS, the SWM drives coastal upwelling off Yemen and Somalia, while the NEM causes convective mixing in its northern part. Both processes bring deep nutrient-rich waters to the surface promoting phytoplankton blooms. While the effects of the reversing monsoons are also prominent in the BoB, the freshwater inputs from the Brahmaputra and Ganges rivers stratify the water column, constraining mixing with nutrient-rich deep waters and hence the development phytoplankton blooms. During the intermonsoon (IM) periods (March–May and October), the IO comes into an oligotrophic transitional state (Jinadasa et al. 2020; Jiang et al. 2022).

We collected all currently available N_2 fixation measurements in the IO for different sub-basins and seasons (Fig. 1, <https://zenodo.org/record/7870536>). Though the number of depth-integrated rates available in the literature is much smaller than that of volumetric rates ($n = 103$ and $n = 246$, respectively; <https://zenodo.org/record/7870536>), due to the marked vertical variability of N_2 fixation in the water column (e.g., Church et al. 2005), depth-integrated rates are more reliable for basin-scale estimations. Summing the seasonal sub-basin contributions of depth-integrated N_2 fixation rates (<https://zenodo.org/record/7870536>), we calculate yearly basin-scale rates of 9.24, 7.54, and 13.57 Tg $N\ yr^{-1}$, based on arithmetic mean, geometric mean, and median, respectively (<https://zenodo.org/record/7870536>). Considering a global N_2 fixation rate estimate of 196.1 Tg $N\ yr^{-1}$ (Tang et al. 2019b), the IO represents 4–7% of the global N_2 fixation inputs. Given that the IO accounts for 22% of the global ocean surface, the calculated contribution of this basin to global N_2 fixation inputs is low. This is likely importantly affected by the uneven seasonal and sub-basin coverage of the measurements published to date, lacking summer measurements in the AS and the EqIO, and winter and IM measurements in the EIO, IOSG, and SIO (<https://zenodo.org/record/7870536>).

Our basin-scale yearly estimates are thus close to the that of Tang et al. (11.5 Tg $N\ yr^{-1}$; Tang et al. 2019a), but are substantially lower than the estimate of Großkopf et al. (26 Tg $N\ yr^{-1}$; Großkopf et al. 2012). The estimate of Großkopf et al. (2012) was based on North Pacific rates applied to the areal surface of the IO, likely leading to overestimation. Our current estimates are instead likely underestimated due to the lack of data in certain sub-basins and seasons, including summer in the AS and EqIO, and winter and IM in the EIO, IOSG and SIO (<https://zenodo.org/record/7870536>).

Below we discuss N_2 fixation and diazotroph community composition geographical and seasonal patterns for each sub-basin separately.

Box 1. Main acronyms used in this review.

AS—Arabian Sea.
BoB—Bay of Bengal.
EIO—eastern Indian Ocean.
EqIO—equatorial Indian Ocean.
IIOE—International Indian Ocean Expedition.
IM—intermonsoon.
IO—Indian Ocean.
IOSG—Indian Ocean subtropical gyre.
NEM—northeast monsoon.
SIO—southern Indian Ocean.
SWM—southwest monsoon.

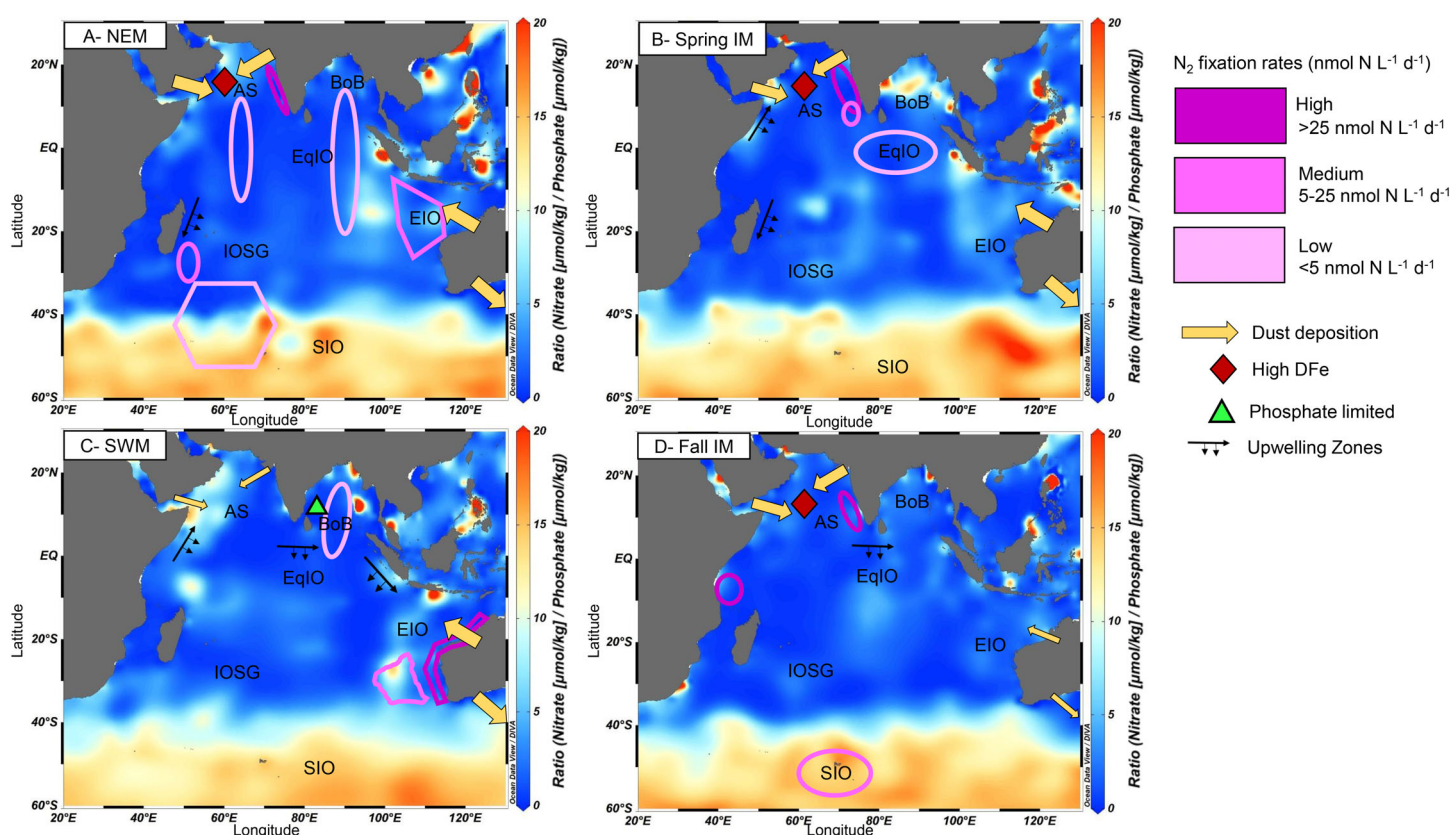


Fig. 1. Schematic representation of the main features controlling N_2 fixation activity and diazotroph diversity in the Indian Ocean overlaid on nitrate-to-phosphate ratios obtained from the World Ocean Atlas 2019 (Boyer et al. 2018) during (A) northeast monsoon (NEM; corresponding to boreal winter/austral summer), (B) spring intermonsoon (spring IM; corresponding to boreal spring and austral winter), (C) southwest monsoon (SWM; corresponding to boreal summer/austral winter), and (D) fall intermonsoon (fall IM; corresponding to boreal fall/austral summer). DFe, dissolved iron.

Arabian Sea

In the landlocked northern IO, the AS and BoB sub-basins are biogeochemically different despite their similar latitudinal range and equal exposure to the monsoon regime (Hood et al. 2007). Currently available N_2 fixation rate measurements in the photic layer of the AS are restricted to the NEM and IM periods. Volumetric N_2 fixation in the AS range from 0.14 to 225.10 $\text{nmol N L}^{-1} \text{d}^{-1}$ and 3 to 528 $\text{nmol N L}^{-1} \text{d}^{-1}$, while depth-integrated rates range from 6.27 to 2500 $\mu\text{mol N m}^{-2} \text{d}^{-1}$ and from 54.5 to 7687.50 $\mu\text{mol N m}^{-2} \text{d}^{-1}$ during the NEM and the IM, respectively (Appendix S1). These ranges exclude the extremely high rates of 15,895 $\mu\text{mol N m}^{-2} \text{d}^{-1}$ measured by Gandhi et al. (2011) inside a dense patch of *Trichodesmium* bloom.

N_2 fixation rates measured during the NEM in the eastern AS are comparable to those measured during the IM (Singh et al. 2019), suggesting that the eastern AS holds biogeochemical conditions favorable for diazotrophy throughout the different seasons (Singh et al. 2019). The highest rates correspond to measurements in coastal regions (Figs. 2, 3) (Gandhi et al. 2011; Ahmed et al. 2017). These high rates may be inflated by high particulate nitrogen biomass, as seen in other coastal systems

(Selden et al. 2019). Previous studies observed *Trichodesmium* blooms in the eastern AS during the spring IM (Capone et al. 1998; Naqvi et al. 2009), which were estimated to provide 15.4 Tg N yr^{-1} to the AS, accounting for 92% of the new nitrogen input to this sub-basin (Gandhi et al. 2011). However, other studies conducted in the same sub-basin during this period argued that NCDs were the major contributors due to high N_2 fixation rates observed in dark incubations as compared to light incubations (Kumar et al. 2017). However, many cyanobacterial diazotrophs such as *Crocosphaera* and *Cyanothece* are known to fix N_2 at night and carbon during the day to avoid deactivation of the nitrogenase enzyme by photosynthesis-derived oxygen (Zehr and Capone 2020).

In the AS, the SWM drives coastal upwelling off Yemen and Somalia, while the NEM causes convective mixing in its northern part (Madhupratap et al. 1996; Naqvi et al. 2008). Both processes alter water column stability bringing deep nutrient-rich waters to the surface and lowering temperature (Madhupratap et al. 1996; Conkright et al. 2000). Such conditions are usually considered deleterious for the proliferation of the filamentous diazotroph *Trichodesmium* (Zehr and Capone 2020), but may not disrupt N_2 fixation in unicellular

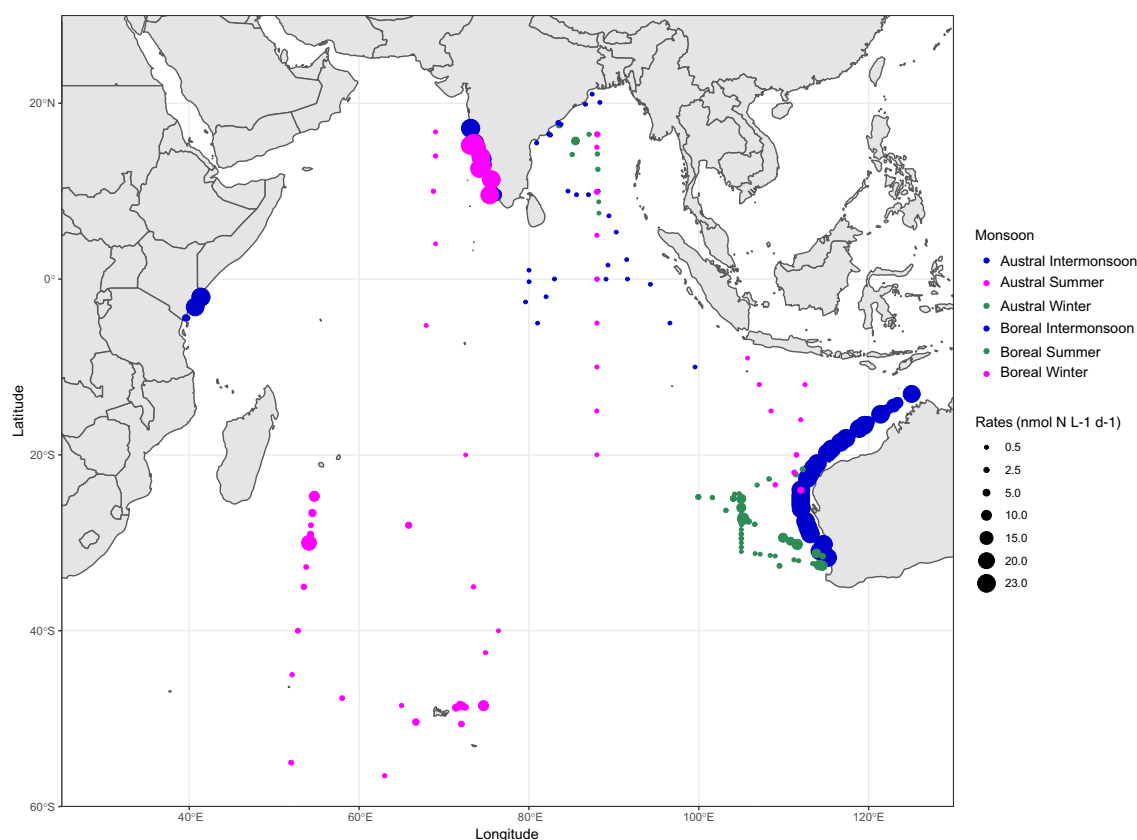


Fig. 2. Volumetric N_2 fixation rates compiled from previously published studies (listed in Appendix S1). Rates $> 23 \text{ nmol N L}^{-1} \text{ d}^{-1}$ are represented as $23 \text{ nmol N L}^{-1} \text{ d}^{-1}$.

cyanobacteria (Mills et al. 2020). While upwelling during the SWM provides reactive nitrogen promoting phytoplankton growth in the eastern AS (Wiggert et al. 2006; Wiggert and Murtugudde 2007; Koné et al. 2009; Resplandy et al. 2009), during the late SWM iron becomes limiting to promote further primary productivity in the region (Measures and Vink 1999; Moffett et al. 2015). Thus, the combination of upwelled nitrate and low relative iron availability may affect N_2 fixation in the eastern AS during the SWM. In turn, during the IM period denitrification and/or non-Redfieldian nitrate utilization creates an excess of phosphorus likely favoring N_2 fixation (Singh et al. 2019). These conditions, along with the important iron-rich atmospheric dust inputs from the surrounding Thar and Arabian deserts (Banerjee and Prasanna Kumar 2014), enhance N_2 fixation in the AS during the IM (Mulholland and Capone 2009; Singh et al. 2019).

Bay of Bengal

The BoB presents lower N_2 fixation rates than the AS (Appendix S1). Surface volumetric N_2 fixation measurements from the BoB have been conducted during the NEM, SWM and IM periods, ranging from below the detection limit to $2.56 \text{ nmol N L}^{-1} \text{ d}^{-1}$ during the NEM, and between 0.13 and

$6.69 \text{ nmol N L}^{-1} \text{ d}^{-1}$ during the SWM (Fig. 2; Appendix S1). Depth-integrated rates range from below the detection limit to $75.61 \mu\text{mol N m}^{-2} \text{ d}^{-1}$ during the NEM, between 4.12 and $75.00 \mu\text{mol N m}^{-2} \text{ d}^{-1}$ during the SWM, and between 0.72 and $14.82 \mu\text{mol N m}^{-2} \text{ d}^{-1}$ (from the coastal BoB) during the IM (Appendix S1), being particularly high in the central BoB than in its northwestern and coastal parts (Fig. 3).

The BoB has a unique biogeochemical signature with respect to the other sub-ocean basins of the IO. Here, significant nutrient riverine phosphorus inputs (Chinni et al. 2019) and high atmospheric iron deposition fluxes ($82.8\text{--}135 \text{ nmol m}^{-2} \text{ d}^{-1}$; Grand et al. 2015), predict an important diazotrophic activity. This is supported by the low $\delta^{15}\text{N}$ values detected in the sediment of the BoB (Gaye-Haake et al. 2005). However, several studies conducted during the NEM and SWM seasons found N_2 fixation rates close to the detection limit (Löscher et al. 2020; Saxena et al. 2020; Sarma et al. 2020). This may be caused by freshwater inputs promoting stratification and restricting vertical nutrient fluxes (Schott and McCreary 2001), and rapid consumption close to the coast leading to phosphorus limitation offshore (Singh and Ramesh 2011). However, more recent studies measured positive values of P^* (the excess of phosphate with respect to NO_3^-

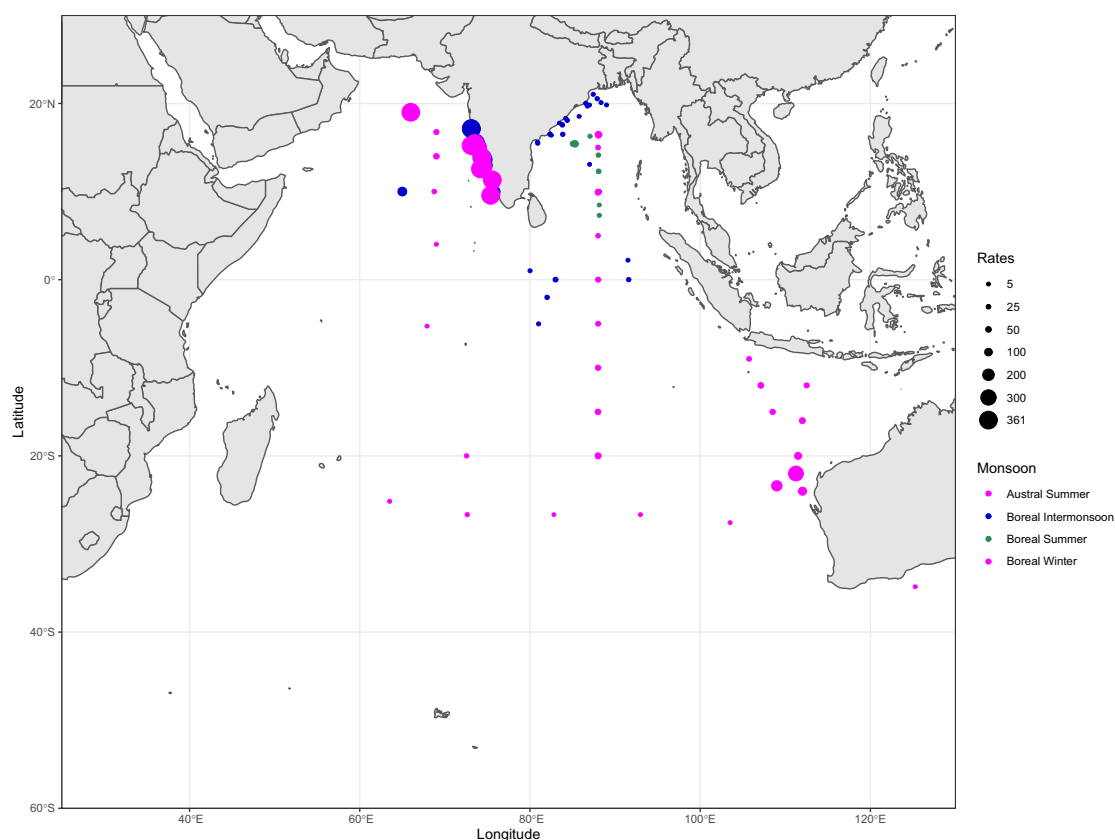


Fig. 3. Depth-integrated N_2 fixation rates compiled from previously published studies (listed in Appendix S1). Rates $> 361 \mu\text{mol N m}^{-2} \text{d}^{-1}$ are represented as $361 \mu\text{mol N m}^{-2} \text{d}^{-1}$.

considering a Redfield ratio; Michaels et al. 1996) and high dissolved iron concentrations ($0.2\text{--}0.5 \text{ nmol L}^{-1}$) which, however, did not visibly result in higher N_2 fixation rates than observed in previous studies (Sato et al. 2022). This may be influenced by time constrained events such as seasonal cyclones and mesoscale features pulsing reactive nitrogen into the euphotic zone and inhibiting the development of diazotrophs (Singh and Ramesh 2015). Alternatively, the low iron to nitrogen (Fe : N) ratio of aerosol inputs has been suggested as a possible explanation for low N_2 fixation activity in the BoB (Sato et al. 2022). A recent study (Saxena et al. in review), argues that the negative effects of turbulence on diazotrophs may override the benefits of favorable nutrient conditions for diazotrophy in the BoB. Linking the frequency of nutrient enriching events such as aeolian inputs, atmospheric cyclones and mesoscale features to the different seasons is needed for a better assessment of the contribution of N_2 fixation in the BoB to overall reactive nitrogen inputs in the IO.

Equatorial Indian Ocean

N_2 fixation rates in the eastern EqIO range from 0.22 to $1.16 \text{ nmol N L}^{-1} \text{d}^{-1}$ during the NEM, and from 0.03 to $0.20 \text{ nmol N L}^{-1} \text{d}^{-1}$ during the IM period (Appendix S1).

Low rates were detected in the central and eastern EqIO during the IM, whereas the rates from the western EqIO are comparatively higher ($0\text{--}173.8 \text{ nmol N L}^{-1} \text{d}^{-1}$) (Figs. 2, 3). Depth-integrated rates range from 8.30 to $40.2 \mu\text{mol N m}^{-2} \text{d}^{-1}$ and from 7.41 to $30.15 \mu\text{mol N m}^{-2} \text{d}^{-1}$ during the NEM and IM periods, respectively (Appendix S1).

At $\sim 0\text{--}10^\circ\text{S}$ in the central EqIO, upwelling promotes important nitrate diffusive fluxes ($46.9\text{--}397 \mu\text{mol m}^{-2} \text{d}^{-1}$) with high N : P ratio values (Sato et al. 2022). Together with the low dissolved iron concentrations of this region (Thi Dieu Vu and Sohrin 2013; Baer et al. 2019), these biogeochemical conditions seem to inhibit diazotrophy in the central EqIO (Sato et al. 2022). In the eastern EqIO N_2 fixation rates are also low ($0.03\text{--}0.20$ and $0.10\text{--}1.16 \text{ nmol N L}^{-1} \text{d}^{-1}$ during the IM and NEM, respectively; Sato et al. 2022, Wu et al. 2019), despite its deep thermocline and nutricline (Murtugudde et al. 1999; Vinayachandran et al. 2009; 2021). In turn, high N_2 fixation rates (up to $173.8 \text{ nmol N L}^{-1} \text{d}^{-1}$) have been observed in the western EqIO, likely attributable to *Trichodesmium* blooms close to the Kenyan coast (Kromkamp et al. 1997). On top of sub-basin geographical and seasonal variability, climatic oscillations such as the IO dipole may control N_2 fixation inputs at longer time scales in the EqIO (Wiggert et al. 2009).

Indian Ocean subtropical gyre

All N_2 fixation measurements in the IOSG have been done during the austral SWM (Appendix S1). Here, surface volumetric N_2 fixation rates range from 0.14 to 18.26 $\text{nmol N L}^{-1} \text{d}^{-1}$ and depth-integrated rates range from 16.6 to 58.2 $\mu\text{mol N m}^{-2} \text{d}^{-1}$, with the higher end of the range corresponding to the northern part of the IOSG (Fig. 2).

The IOSG is one of the world's five wide oligotrophic gyres where phosphorus and reactive nitrogen concentrations are at or below the detection limit (Harms et al. 2019; Geisen et al. 2022). The IOSG N_2 fixation rates available thus far do not correlate with nutrient concentrations nor with temperature (Hörstmann et al. 2021). In the central IOSG, N_2 fixation rates reach up to 7.93 $\text{nmol N L}^{-1} \text{d}^{-1}$ (Appendix S1). Comparatively higher rates up to 18.3 $\text{nmol N L}^{-1} \text{d}^{-1}$ have been reported from the western flank of the IOSG, associated with *Trichodesmium* blooms off Madagascar (Poulton et al. 2009; Metzl et al. 2022). In all, the IOSG remains as the IO's sub-basin with the least measurements available, and thus a priority for future research efforts.

Eastern Indian Ocean

Surface N_2 fixation rates in the EIO range from 0.17 to 52.35 $\text{nmol N L}^{-1} \text{d}^{-1}$ during the austral summer (November–March), from 0 to 77.89 $\text{nmol N L}^{-1} \text{d}^{-1}$ during austral IM (April–May, October), and from 0.2 to 12.64 $\text{nmol N L}^{-1} \text{d}^{-1}$ during the austral winter (June–September). Depth-integrated N_2 fixation rates down to 160 m have been only measured in the eastern side of the EIO during the austral summer, where they range from 26.1 to 286 $\mu\text{mol N m}^{-2} \text{d}^{-1}$ (Appendix S1).

In austral summer, the Indian Ocean Dipole induces a positive sea surface anomaly in the western coast of Australia (Terry et al. 2005), which together with iron-rich dust deposition from the Australian landmass is thought to promote relatively high N_2 fixation rates during the austral IM (up to 77.89 $\text{nmol N L}^{-1} \text{d}^{-1}$), despite the concomitant notable upward nitrate fluxes (Raes et al. 2015; Sato et al. 2022). The highest nitrate concentrations in this region are, however, found during the austral winter (up to 0.8 $\mu\text{mol L}^{-1}$). Such enrichment is thought to be due to the strengthening of the Leeuwin current in winter eroding the nutricline and increasing nitrate concentrations at the surface (Feng et al. 2003). This nitrate enrichment could be responsible for lower N_2 fixation rates in the austral winter as compared to austral IM and summer (Raes et al. 2015).

Southern Indian Ocean

Surface N_2 fixation rates in the SIO range from 0.78 to 10.27 $\text{nmol N L}^{-1} \text{d}^{-1}$ during austral summer (November–March). No depth-integrated N_2 fixation measurements are available from this region of the IO. Integrating surface volumetric N_2 fixation rates down to 80 m, we obtain rates ranging from 62.40 to 157.60 $\mu\text{mol N m}^{-2} \text{d}^{-1}$ (Appendix S1). The SIO connects to the Southern Ocean, one of the most important high nutrient-low chlorophyll zones in the world's

oceans (Venables and Moore 2010). Here, primary productivity remains low due to chronic iron limitation (Martin et al. 1990), which together with high nitrate availability presents unfavorable conditions for N_2 fixation (Zehr and Capone 2020). However, certain regions of the SIO present measurable N_2 fixation rates (0.78–10.27 $\text{nmol N L}^{-1} \text{d}^{-1}$; González et al. 2014; Hörstmann et al. 2021).

Distribution and diversity of diazotrophs in the Indian Ocean

N_2 fixation is mediated by the nitrogenase enzyme complex, which contains the proteins dinitrogenase and the dinitrogenase reductase, encoded by the *nifDK* and *nifH* genes, respectively (Burgess and Lowe 1996). The *nifH* gene is widely used in diazotrophy research as it has been highly conserved throughout evolution, being an easy target for downstream molecular analyses (Zehr et al. 2003). It must be noted that the *nifH* amplicon or Sanger sequencing-based analyses target only one out of the six genes needed for N_2 fixation to occur, which may lead to biased interpretations of the potentially active diazotrophic community and how it is linked to bulk N_2 fixation rate measurements (Delmont et al. 2022). However, several sequences detected in the AS displayed the full *nifHDKENB* operon (Jayakumar et al. 2012; Bird and Wyman 2013; Jayakumar and Ward 2020).

Most of our knowledge on diazotroph community composition in the IO stems from a limited number of next-generation sequencing datasets (Raes et al. 2018; Wu et al. 2019; Li et al. 2021; Wu et al. 2021; Sato et al. 2022; Table S1), cloning-based *nifH* Sanger sequencing studies from the AS, BoB, and EIO (Mazard et al. 2004; Bird et al. 2005; Jayakumar et al. 2012; Bird and Wyman 2013; Shiozaki et al. 2014; Löscher et al. 2020; Table S2), and a few quantitative PCR (qPCR) *nifH* gene counts (Shiozaki et al. 2014; Löscher et al. 2020; Sato et al. 2022; Fig. S1). Our compilation of published *nifH* gene-based molecular data shows a dominance of gammaproteobacteria (Fig. 4), as observed in other larger-scale ocean studies (Farnelid et al. 2011; Delmont et al. 2022). However, it must be noted that compositional data is not quantitative, and *nifH* gene PCR assays are prone to an overrepresentation of gammaproteobacteria (Zehr et al. 2003). Key cyanobacterial diazotrophs such as *Trichodesmium* are mostly present in the AS and BoB under favorable conditions (i.e., iron inputs, low nitrate, high temperature) occurring mostly during the NEM and IM seasons. Unicellular cyanobacterial diazotrophs such as UCYN-A are mostly present in the eastern EIO (Appendix S2; Fig. S1), but not commonly detected in the western EIO despite the favorable biogeochemical conditions (Shiozaki et al. 2014; Sato et al. 2022). The relatively high N_2 fixation rates along with the dominance of NCD sequences in the western EIO and the EqIO (Wu et al. 2019, 2021; Hörstmann et al. 2021), suggest an important contribution of NCDs to nitrogen inputs in this

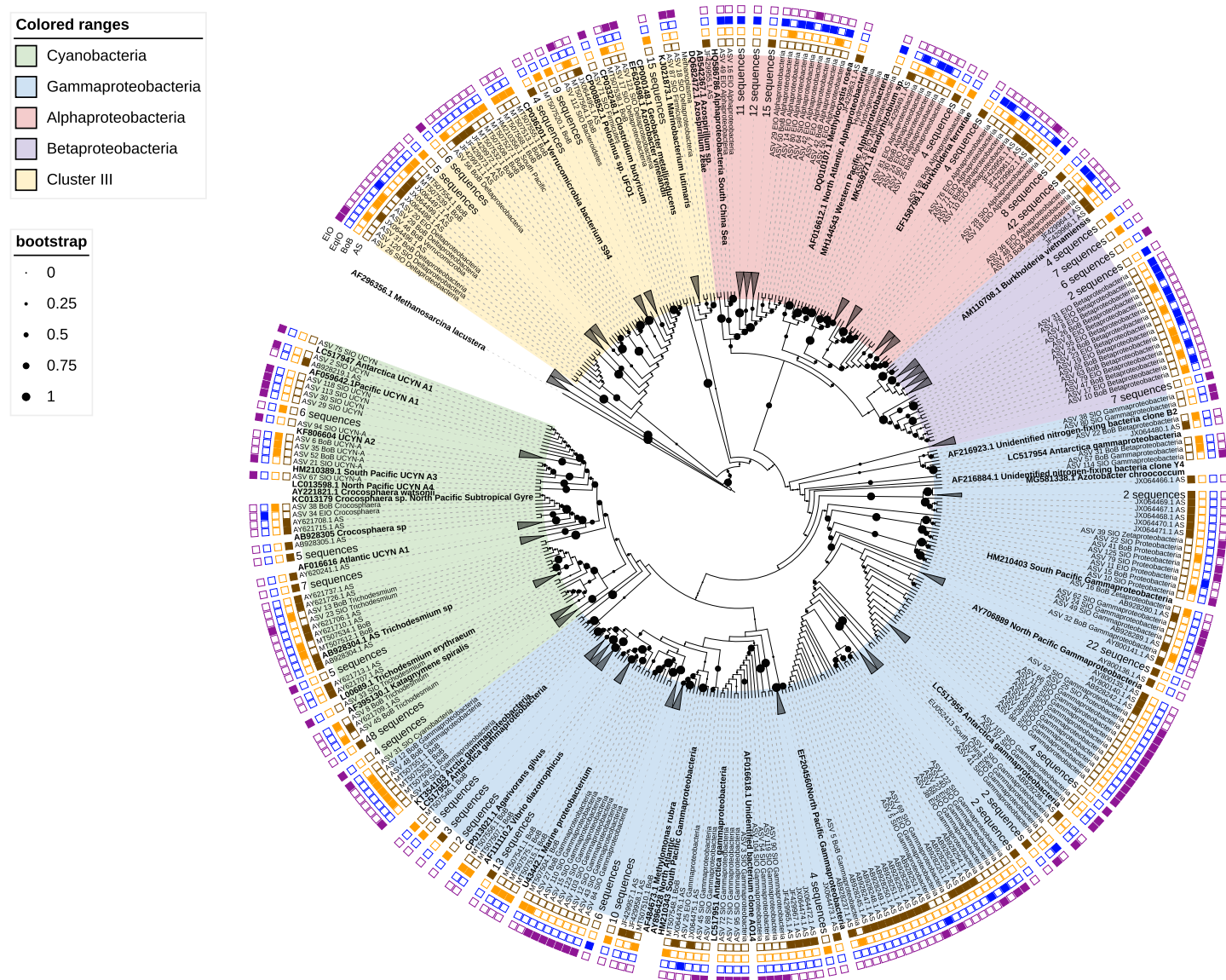


Fig. 4. Maximum likelihood phylogenetic tree representing diazotroph diversity in the Indian Ocean. The tree was built using ASVs (occurrences > 1000) from *nifH* amplicon sequencing and cloning sequences from the studies listed in Appendix S2. The outer rings show the detection of ASVs in different IO sub-basins.

region. However, currently no method exists to measure NCD N_2 fixation alone reliably, and the concomitant presence of cyanobacterial diazotrophs likely mask their activity (Benavides et al. 2022).

Our analyses also show that the diazotroph communities in the BoB, EqIO, and EIO are remarkably different from each other (Fig. 4; Appendix S2; Figs. S3–S6) and subject to seasonal variability driven by the changing monsoons (Appendix S2; Figs. S3–S6). Examining the overlap of diazotroph communities at the order and family level, we find less similarity between the EqIO and the BoB (23 overlapping taxa at the order level, and 31 overlapping taxa at the family level; Fig. 5). This suggests that spatially close

regions can harbor very distinct community compositions, suggesting a high degree of endemism in the IO's diazotroph communities. This is supported by an ANOSIM test showing that *nifH* sequences are significantly different among sub-basins (ANOSIM statistic R : 0.5272, n = 94, p = 0.001) but not among seasons. Such differences are likely caused by physical barriers introduced by ocean dynamics (Hörstmann et al. 2021). However, the sparse spatiotemporal distribution of data available to date may be misinterpreted as endemism. Details regarding the diazotroph community composition and their distribution on the different IO sub-basins according to the data published to date are discussed in the next sections.

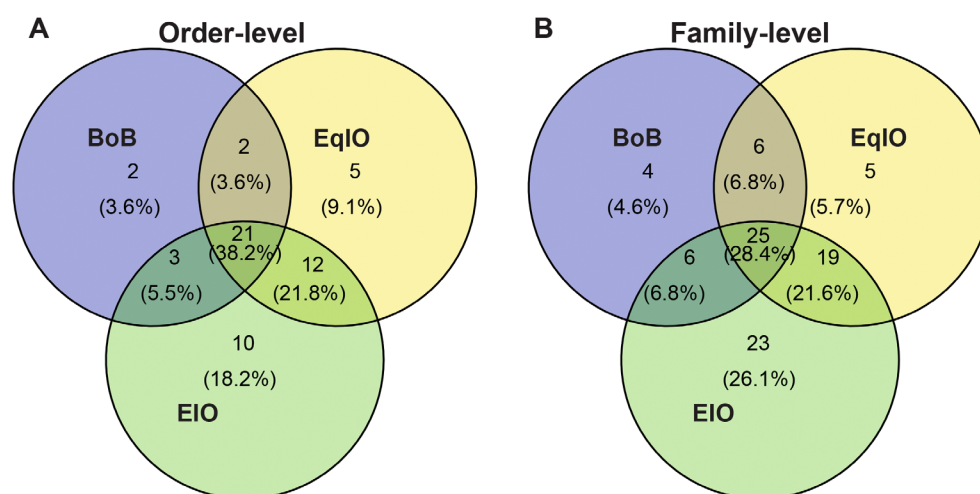


Fig. 5. Venn diagrams of individual and overlapping ASVs on the (A) order level, and (B) family level between regions discussed in this review including the Bay of Bengal (BoB), Equatorial Indian Ocean (EqIO), and Eastern Indian Ocean (EIO). The AS, IOSG, and the SIO are not represented here as there are no *nifH* amplicon sequencing data available from these sub-basins.

Arabian Sea

The AS holds one of the world's most prominent OMZs (Lachkar et al. 2019). Above and within this OMZ, diverse NCDs including proteobacterial diazotrophs (alpha-, beta-, and gammaproteobacteria), as well as cluster II, III, and IV diazotrophs, have been reported (Jayakumar et al. 2012; Jayakumar and Ward 2020). In the AS, NCDs are seemingly not inhibited by reactive nitrogen availability, in contrast with most cyanobacterial diazotrophs (Bird et al. 2005; Bird and Wyman 2013). Despite the relative dominance of NCDs in the AS and the detection of their *nifH* genes at the RNA level, the lack of significant N_2 fixation rates within the AS OMZ questions their contribution to fixed nitrogen inputs (Jayakumar and Ward 2020).

During the NEM, high temperatures and low inorganic nitrogen availability in the central and western AS favor the development of cyanobacterial diazotrophs including UCYN-B, UCYN-C (Mazard et al. 2004), *Trichodesmium* and *Katagnymene* (Bird and Wyman 2013). During the SWM nitrate upwelling appears to favor the development of UCYN-B over *Trichodesmium* (Shiozaki et al. 2014) (Fig. 4). In the central AS, the detection of NCD *nifH* sequences at both the DNA and RNA level in the absence of cyanobacterial diazotroph sequences along with relatively high N_2 fixation rates suggests that NCDs actively fix N_2 (Shiozaki et al. 2014), which awaits confirmation with NCD-specific N_2 fixation assays yet to be developed (Turk-Kubo et al. 2022).

Bay of Bengal

The diazotroph community of the BoB comprises eight phyla (Appendix S2; Fig. S2). The main representatives NCDs from the BoB include gammaproteobacteria (*Amphritea*, *Agarivorans*, *Marinobacterium*, *Pseudomonas*, *Succinivibrio*,

Vibrio, *Teredinibacter*), betaproteobacteria (*Aquaspirillum*, *Azohydromonas*, *Propionivibrio*, *Methyloversatilis*), and alphaproteobacteria (*Bosea*, *Bradyrhizobium*, *Methylocystis*, *Novosphingobium*, *Xanthobacter*). Regarding cyanobacterial diazotrophs, studies conducting *nifH* amplicon sequencing and qPCR analyses reported a higher abundance of *Trichodesmium* than of unicellular cyanobacteria groups (Appendix S2; Fig. S1; Wu et al. 2019, 2021). At the seasonal variability level, in the BoB the IM season seems to favor cyanobacterial diazotrophs while the NEM rather supports NCDs. However, such trends are hard to evaluate based on compositional data, and quantitative approaches covering a wider diazotroph diversity are needed.

During the IM, cyanobacterial diazotrophs are dominant both in terms of *nifH* amplicon and qPCR counts, and positively correlated with chlorophyll concentrations (Wu et al. 2019). During the NEM, gamma-, beta- and alphaproteobacteria are abundant in surface waters of the BoB (Appendix S2; Fig. S3). In other seasons, the BoB harbors cyanobacterial representatives including *Trichodesmium* (particularly during the IM), *Richelia*, *Katagnymene*, UCYN-A, and UCYN-B. Because *Trichodesmium* typically grows in oligotrophic and stratified epipelagic waters (Capone et al. 1997), the high turbulence and strong wind conditions observed in the BoB during the NEM and SWM may be unfavorable for their growth (Wu et al. 2022). While cyanobacteria predominate at the surface, alpha- and betaproteobacteria are significantly more abundant at deeper levels (based on the relative abundance of ASVs) (Appendix S2; Fig. S6; Wu et al. 2022).

During the NEM, cyanobacteria and gammaproteobacteria are relatively abundant in the surface of the central BoB while beta- and alphaproteobacteria are more abundant in the south (Appendix S2; Fig. S3). A recent study showed that

gammaproteobacterial diazotrophs are negatively influenced by temperature during the NEM in the BoB and positively correlated with silicate, suggesting a possible association with diatoms (Shao and Luo 2022). Instead, in the BoB alpha- and betaproteobacterial diazotrophs are positively correlated to temperature (Wu et al. 2022).

More recent qPCR studies have either detected (Li et al. 2021) or not detected (Sato et al. 2022) UCYN-A during the NEM, which may imply interannual variability in the composition of the diazotroph community for reasons yet to be understood. The southern edge of the BoB features anticyclonic eddies along 10° N during the IM period leading to strong water column stratification and oligotrophic conditions, favoring cyanobacterial diazotroph growth (Jyothibabu et al. 2017; Wu et al. 2021).

Equatorial Indian Ocean

Among the cyanobacterial diazotrophs detected in the EqIO, we found more ASVs annotated as *Trichodesmium*, while UCYN-A was represented only by two ASVs out of the 87 cyanobacterial ASVs retrieved from this sub-basin. However, our analysis reveals that NCDs dominate the diazotroph community in the EqIO, with alphaproteobacteria being the most prominent group, followed by gammaproteobacteria, betaproteobacteria, and cyanobacteria, while some gammaproteobacteria and cluster III groups have been detected at the RNA level in the EqIO (Bird and Wyman 2013) (Fig. 4; Appendix S2; Fig. S4). Particularly, the diazotroph community of the EqIO consists of ten phyla (Appendix S2; Fig. S2). Major NCDs like gammaproteobacterial groups (*Amphritea*, *Pseudomonas*, *Vibrio*, *Teredinibacter*, *Marinobacter*), betaproteobacteria (*Aquaspirillum*, *Aquabacterium*, *Azohydromonas*, *Methyloversatilis*, *Propionivibrio*), and alphaproteobacteria (*Azorhizobium*, *Bradyrhizobium*, *Bosea*, *Caenispirillum*, *Magnetovibrio*, *Methylocystis*, *Novosphingobium*, *Xanthobacter*, *Yangia*) have been detected in the EqIO. Some seasonal patterns emerge, with gammaproteobacteria being more abundant during NEM and early to late IM (Appendix S2; Figs. S4, S5), and alphaproteobacteria more abundant during the IM (Appendix S2; Fig. S4). Detectable rates in the absence of cyanobacterial diazotrophs have been interpreted as a significant contribution of NCDs N₂ fixation rates during the IM in the EqIO (Wu et al. 2019, 2021). Just as in the other sub-basins where NCDs dominate, it is yet unclear if and how these diazotrophs contribute to fixed nitrogen inputs and how they obtain energy to fix N₂. Recent analyses of NCDs metagenome assembled genomes show a variety of possible energy obtaining metabolisms, including anoxygenic photosynthesis, dissimilatory sulfate reduction, thiosulfate oxidation, dissimilatory nitrate reduction and denitrification (Turk-Kubo et al. 2022).

During the IM, the diazotroph community is comprised of alpha-, beta-, and gammaproteobacteria, with high relative abundance of gammaproteobacteria, followed by cyanobacteria

and betaproteobacteria (Appendix S2; Fig. S5). There is then a community shift (intra-seasonal variations) even within the same monsoon period at the EqIO. In all, the NEM appears to favor the growth of limited cyanobacterial diazotrophs, whereas, during IM NCDs dominate in the EqIO. Overall, the NEM appears to support a limited number of cyanobacterial diazotrophs, whereas during the IM NCDs dominate in the EqIO.

Indian Ocean subtropical gyre

The IOSG is by far the IO's sub-basin with the least *nifH* data available (Fig. 1), which precludes us from including any sequences in the phylogenetic tree shown in Fig. 4. The few studies conducted found diatom-diazotroph associations (DDAs) to the southwest of the IOSG, in agreement with previous reports (Pierella Karlusich et al. 2021; Metzl et al. 2022). DDAs in this region are probably related to phosphorus and trace metal weathering off Madagascar island (Baer et al. 2019). However, we note that DDAs are not properly amplified by the usual *nifH* amplicon analysis procedure (Turk-Kubo et al. 2012), which may downplay the role of these diazotrophs in the IO. Further offshore in the central IOSG where island delivered nutrients are not available, smaller diazotrophs such as UCYN-A and NCDs may dominate, but this remains a mere speculation at this stage.

Southern Indian Ocean

The EIO also shows a relative dominance of NCDs (Appendix S2; Figs. S2, S7). Major NCDs detected from the EIO include gammaproteobacteria (*Achromatium*, *Agarivorans*, *Klebsiella*, *Methyloprofundus*, *Sedimenticola*, *Teredinibacter*, *Vibrio*), betaproteobacteria (*Aquaspirillum*, *Ferriphaselus*, *Formivibrio*, *Sulfuriferula*, *Sulfuricella*, *Propionivibrio*), and alphaproteobacteria (*Caenispirillum*, *Cohaesibacter*, *Magnetovibrio*, *Novosphingobium*). The sequences annotated as deltaproteobacteria genera *Desulfovibrio* and *Desulfocarbo* with putative sulfate-reducing mechanisms are more frequently detected in the EIO than in the BoB or the EqIO (Fig. 4).

Gammaproteobacteria predominate during the austral summer, followed by *Clostridia* and cyanobacteria (particularly during the IM; Appendix S2; Fig. S7). Low temperatures in the EIO may favor NCDs over cyanobacterial diazotrophs (Qin et al. 2014). Metagenome analysis from the EIO revealed gammaproteobacteria to be the dominant class (Wang et al. 2021), which is consistent with *nifH* amplicon data in this sub-basin (Fig. 4).

At lower latitudes such as the northern part of Australia and the Timor Sea, cyanobacterial diazotrophs such as *Trichodesmium* are more abundant, while UCYN-A is the main suspect for the relatively high rates observed in the western coast of Australia (Raes et al. 2014). This is supported by the observations of Sato et al. (2022), who detected higher abundances of UCYN-A than *Trichodesmium* coinciding with increased N₂ fixation rates (Appendix S2; Fig. S1).

Knowledge gaps and future perspectives of N_2 fixation research in the Indian Ocean: A strong seasonal signature

The monsoon system is widely recognized to impact the climate and biogeochemistry of the IO (Hood et al. 2009; Hermes et al. 2019). However, the N_2 fixation rate data available thus far for the IO are not evenly distributed among seasons (Appendix S1; Fig. 2), which hampers making accurate nitrogen budgets for the whole basin. In the AS N_2 fixation measurements have been focused on the NEM and IM periods, covering the eastern and central parts of this sub-basin. However, there are no N_2 fixation rate measurements in the AS during the SWM period, and the western AS remains totally unexplored (Fig. 2). As compared to the AS, the BoB has more N_2 fixation data coverage, with all the monsoon periods represented (SWM, NEM, and IM). In the EqIO, N_2 fixation has only been measured during the NEM and IM periods (Fig. 2). Comparing studies in the EIO reveals that the austral IM induces higher N_2 fixation activity than the austral summer or winter seasons. The seasonality of N_2 fixation activity in the IOSG remains difficult to assess because data is only available for the austral SWM period (Appendix S1; Fig. 2).

Our data compilation indicates that the conditions induced by the NEM and the IM periods are favorable for diazotrophy in the northern IO, whereas the austral IM is likely more influential in the EIO. An analysis of the standard deviation by surface of each sub-basin reveals that N_2 fixation rates are more variable in the BoB, AS and EIO. In the case of the northern IO sub-basins (BoB and AS), N_2 fixation seems driven by high seasonal variability governed by the reversing monsoon system. In the particular case of the AS, there is a strong spatial bias in the measurements where most depth-integrated rates available come from coastal areas (Fig. 3). In the case of the EIO, the depth-integrated N_2 fixation rates are few (11 values published in Fernández-Castro et al. 2015 and Sato et al. 2022; Appendix S1) and covering a wide range of rates ($4.5\text{--}170\ \mu\text{mol m}^{-2}\text{ d}^{-1}$). Hence, a better spatially resolved sampling is needed in the EIO.

Particularly, we identify the SWM in the AS, the NEM in the BoB, the SWM in the EqIO, and both the austral winter and austral IM in the IOSG as the main seasonal/geographical coverage currently lacking to improve our understanding of the monsoon's impact on N_2 fixation rates in the IO. The spatial and seasonal heterogeneity of the IO's sub-basins in terms of aeolian dust deposition and inorganic nutrient availability plead for thorough seawater chemical analyses along with N_2 fixation measurements in the future.

Regarding diazotroph community composition, most *nifH* amplicon sequencing studies have been conducted during the NEM and IM periods in the BoB, EqIO, and EIO (Appendix S2; Table S1), while there are no *nifH* sequencing studies available from the AS and the IOSG (Appendix S2; Table S1; sub-basins thus not included in Fig. 5). Our *nifH* sequence compilation

reveals that cyanobacterial diazotrophs prevail during the IM in BoB, while NCDs dominate during the IM in the EqIO and the EIO. To better understand the seasonal effects on diazotroph community composition in the different sub-basins we need further sequencing in the AS (all seasons), the BoB (SWM period), EqIO (SWM period), EIO (austral winter), and all the seasons in the IOSG. The few available quantitative studies (*nifH* qPCR counts) are restricted to the NEM and austral summer monsoon periods, which prevents us from drawing any conclusions on the role of seasons on diazotroph abundance. The high degree of diazotroph community uniqueness among sub-basins (Fig. 5) pleads for genomic and transcriptomic studies able to decipher how different diazotrophs adapt to seasonally changing conditions. In this sense, strain isolation would enable deeper metabolic and phenotypic studies to reveal what factors this unique sub-basin community composition responds to. Moreover, as in other basins of the world's oceans, top-down controls on diazotroph communities remain largely unknown (Landolfi et al. 2021), while they are predicted to impact diazotroph biomass and derived N_2 fixation rates crucially (Wang et al. 2019).

The geographical and seasonal coverage gaps identified here provide a framework for future diazotrophy studies in the IO. Programmes such as the IIOE-2 and the Indian Ocean Observing System (IndOOS-2) provide solid schemes to pursue such measurements and better constrain the role of the IO in global nitrogen cycling. While these programs are mostly focused on the northern IO, we encourage the diazotroph research community to dedicate their future IO work on the EqIO, IOSG and SIO.

References

- Ahmed, A., M. Gauns, S. Kurian, P. Bardhan, A. Pratihary, H. Naik, D. M. Shenoy, and S. W. A. Naqvi. 2017. Nitrogen fixation rates in the eastern Arabian Sea. *Estuar. Coast. Shelf Sci.* **191**: 74–83. doi:10.1016/j.ecss.2017.04.005
- Baer, S. E., S. Rauschenberg, C. A. Garcia, N. S. Garcia, A. C. Martiny, B. S. Twining, and M. W. Lomas. 2019. Carbon and nitrogen productivity during spring in the oligotrophic Indian Ocean along the GO-SHIP IO9N transect. *Deep-Sea Res. II: Top. Stud. Oceanogr.* **161**: 81–91. doi:10.1016/j.dsr2.2018.11.008
- Banerjee, P., and S. Prasanna Kumar. 2014. Dust-induced episodic phytoplankton blooms in the Arabian Sea during winter monsoon. *J. Geophys. Res.: Oceans* **119**: 7123–7138. doi:10.1002/2014JC010304
- Benavides, M., and others. 2022. Sinking *Trichodesmium* fixes nitrogen in the dark ocean. *ISME J.* **16**: 2398–2405. doi:10.1038/s41396-022-01289-6
- Bertagnolli, A. D., and F. J. Stewart. 2018. Microbial niches in marine oxygen minimum zones. *Nat. Rev. Microbiol.* **16**: 723–729. doi:10.1038/s41579-018-0087-z

- Bird, C., J. Martinez Martinez, A. G. O'Donnell, and M. Wyman. 2005. Spatial distribution and transcriptional activity of an uncultured clade of planktonic diazotrophic γ -proteobacteria in the Arabian Sea. *Appl. Environ. Microbiol.* **71**: 2079–2085. doi:[10.1128/AEM.71.4.2079-2085.2005](https://doi.org/10.1128/AEM.71.4.2079-2085.2005)
- Bird, C., and M. Wyman. 2013. Transcriptionally active heterotrophic diazotrophs are widespread in the upper water column of the Arabian Sea. *FEMS Microbiol. Ecol.* **84**: 189–200. doi:[10.1111/1574-6941.12049](https://doi.org/10.1111/1574-6941.12049)
- Bonnet, S., M. Caffin, H. Berthelot, and T. Moutin. 2017. Hot spot of N₂ fixation in the western tropical South Pacific pleads for a spatial decoupling between N₂ fixation and denitrification. *Proc. Natl. Acad. Sci. USA* **114**: E2800–E2801. doi:[10.1073/pnas.1619514114](https://doi.org/10.1073/pnas.1619514114)
- Boyer, T. P., and others. 2018. World Ocean Atlas 2018. [nitrate and phosphate]. NOAA National Centers for Environmental Information. Dataset, [13th December 2022]. Available from <https://www.ncei.noaa.gov/archive/accession/NCEI-WOA18>
- Branagan, D. F. 1972. The challenger expedition and Australian science. *Proc. R. Soc. B: Biol. Sci.* **73**: 85–95. doi:[10.1017/S0080455X00002150](https://doi.org/10.1017/S0080455X00002150)
- Brandes, J. A., and A. H. Devol. 2002. A global marine-fixed nitrogen isotopic budget: Implications for Holocene nitrogen cycling. *Glob. Biogeochem. Cycles* **16**: 67–1–67–14. doi:[10.1029/2001GB001856](https://doi.org/10.1029/2001GB001856)
- Burgess, B. K., and D. J. Lowe. 1996. Mechanism of molybdenum nitrogenase. *Chem. Rev.* **96**: 2983–3012. doi:[10.1021/cr950055x](https://doi.org/10.1021/cr950055x)
- Capone, D. G., J. P. Zehr, H. W. Paerl, B. Bergman, and E. J. Carpenter. 1997. *Trichodesmium*, a globally significant marine cyanobacterium. *Science* **276**: 1221–1229. doi:[10.1126/science.276.5316.1221](https://doi.org/10.1126/science.276.5316.1221)
- Capone, D. G., A. Subramaniam, J. P. Montoya, M. Voss, C. Humborg, A. M. Johansen, R. L. Siefert, and E. J. Carpenter. 1998. An extensive bloom of the N₂-fixing cyanobacterium *Trichodesmium erythraeum* in the central Arabian Sea. **172**: 281–292. doi:[10.3354/meps172281](https://doi.org/10.3354/meps172281)
- Carlson, C. A., P. A. Del Giorgio, and G. J. Herndl. 2007. Microbes and the dissipation of energy and respiration: From cells to ecosystems. *Oceanography* **20**: 89–100. doi:[10.5670/oceanog.2007.52](https://doi.org/10.5670/oceanog.2007.52)
- Cheng, L., and others. 2022. Another record: Ocean warming continues through 2021 despite La Niña conditions. *Adv. Atmos. Sci.* **39**: 373–385. doi:[10.1007/s00376-022-1461-3](https://doi.org/10.1007/s00376-022-1461-3)
- Chinni, V., S. K. Singh, R. Bhushan, R. Rengarajan, and V. V. S. S. Sarma. 2019. Spatial variability in dissolved iron concentrations in the marginal and open waters of the Indian Ocean. *Mar. Chem.* **208**: 11–28. doi:[10.1016/j.marchem.2018.11.007](https://doi.org/10.1016/j.marchem.2018.11.007)
- Church, M. J., B. D. Jenkins, D. M. Karl, and J. P. Zehr. 2005. Vertical distributions of nitrogen-fixing phylotypes at Stn ALOHA in the oligotrophic North Pacific Ocean. *Aquat. Microb. Ecol.* **38**: 3–14.
- Codispoti, L. A. 2007. An oceanic fixed nitrogen sink exceeding 400 Tg N a⁻¹ vs the concept of homeostasis in the fixed-nitrogen inventory. *Biogeosciences* **4**: 233–253. doi:[10.5194/bg-4-233-2007](https://doi.org/10.5194/bg-4-233-2007)
- Conkright, M. E., W. W. Gregg, and S. Levitus. 2000. Seasonal cycle of phosphate in the open ocean. *Deep-Sea Res. I: Oceanogr. Res. Pap.* **47**: 159–175. doi:[10.1016/S0967-0637\(99\)00042-4](https://doi.org/10.1016/S0967-0637(99)00042-4)
- Dekazemacker, J., S. Bonnet, O. Grosso, T. Moutin, M. Bressac, and D. G. Capone. 2013. Evidence of active dinitrogen fixation in surface waters of the eastern tropical South Pacific during El Niño and La Niña events and evaluation of its potential nutrient controls. *Glob. Biogeochem. Cycles* **27**: 768–779. doi:[10.1002/gbc.20063](https://doi.org/10.1002/gbc.20063)
- Delmont, T. O., and others. 2022. Heterotrophic bacterial diazotrophs are more abundant than their cyanobacterial counterparts in metagenomes covering most of the sunlit ocean. *ISME J.* **16**: 927–936. doi:[10.1038/s41396-021-01135-1](https://doi.org/10.1038/s41396-021-01135-1)
- Deutsch, C., J. L. Sarmiento, D. M. Sigman, N. Gruber, and J. P. Dunne. 2007. Spatial coupling of nitrogen inputs and losses in the ocean. *Nature* **445**: 163–167. doi:[10.1038/nature05392](https://doi.org/10.1038/nature05392)
- Devassy, V. P., P. M. A. Bhattathiri, and S. Z. Qasim. 1978. *Trichodesmium* phenomenon. *Indian J. Mar. Sci.* **7**: 168–186.
- Dugdale, R. C., J. J. Goering, and J. H. Ryther. 1964. High nitrogen fixation rates in the Sargasso Sea and the Arabian Sea. *Limnol. Oceanogr.* **9**: 507–510. doi:[10.4319/lo.1964.9.4.0507](https://doi.org/10.4319/lo.1964.9.4.0507)
- Farnelid, H., and others. 2011. Nitrogenase gene amplicons from global marine surface waters are dominated by genes of non-cyanobacteria. *PloS One* **6**: e19223. doi:[10.1371/journal.pone.0019223](https://doi.org/10.1371/journal.pone.0019223)
- Feng, M., G. Meyers, A. Pearce, and S. Wijffels. 2003. Annual and interannual variations of the Leeuwin current at 32°S. *J. Geophys. Res.: Oceans* **108**. doi:[10.1029/2002JC001763](https://doi.org/10.1029/2002JC001763)
- Fernandez, C., M. L. González, C. Muñoz, V. Molina, and L. Farias. 2015. Temporal and spatial variability of biological nitrogen fixation off the upwelling system of central Chile (35–38.5°S). *J. Geophys. Res.: Oceans* **120**: 3330–3349. doi:[10.1002/2014JC010410](https://doi.org/10.1002/2014JC010410)
- Fernández-Castro, B., and others. 2015. Importance of salt fingering for new nitrogen supply in the oligotrophic ocean. *Nat. Commun.* **6**: 8002. doi:[10.1038/ncomms9002](https://doi.org/10.1038/ncomms9002)
- Fernandez, C., L. Farias, and O. Ulloa. 2011. Nitrogen fixation in denitrified marine waters. *PLoS One* **6**: e20539. doi:[10.1371/journal.pone.0020539](https://doi.org/10.1371/journal.pone.0020539)
- Gandhi, N., A. Singh, S. Prakash, R. Ramesh, M. Raman, M. S. Sheshshayee, and S. Shetye. 2011. First direct measurements of N₂ fixation during a *Trichodesmium* bloom in the

- eastern Arabian Sea: N₂ fixation in the Arabian Sea. *Glob. Biogeochem. Cycles* **25**. doi:[10.1029/2010GB003970](https://doi.org/10.1029/2010GB003970)
- Gaye-Haake, B., and others. 2005. Stable nitrogen isotopic ratios of sinking particles and sediments from the northern Indian Ocean. *Mar. Chem.* **96**: 243–255. doi:[10.1016/j.marchem.2005.02.001](https://doi.org/10.1016/j.marchem.2005.02.001)
- Geisen, C., and others. 2022. Phytoplanktonic response to simulated volcanic and desert dust deposition events in the south Indian and southern oceans. *Limnol. Oceanogr.* **67**: 1537–1553. doi:[10.1002/lno.12100](https://doi.org/10.1002/lno.12100)
- González, M. L., V. Molina, L. Florez-Leiva, L. Oriol, A. J. Cavagna, F. Dehairs, L. Farias, and C. Fernandez. 2014. Nitrogen fixation in the Southern Ocean: A case of study of the Fe-fertilized Kerguelen region (KEOPS II cruise). *Biogeosci. Discuss.* **11**: 17151–17185. doi:[10.5194/bgd-11-17151-2014](https://doi.org/10.5194/bgd-11-17151-2014)
- Grand, M. M., and others. 2015. Dissolved Fe and Al in the upper 1000 m of the eastern Indian Ocean: A high-resolution transect along 95°E from the Antarctic margin to the Bay of Bengal. *Glob. Biogeochem. Cycles* **29**: 375–396. doi:[10.1002/2014GB004920](https://doi.org/10.1002/2014GB004920)
- Großkopf, T., and others. 2012. Doubling of marine dinitrogen-fixation rates based on direct measurements. *Nature* **488**: 361–364. doi:[10.1038/nature11338](https://doi.org/10.1038/nature11338)
- Gruber, N. 2008. The marine nitrogen cycle: Overview and challenges, p. 1–50. In D. G. Capone, D. A. Bronk, M. R. Mulholland, and E. J. Carpenter [eds.], *Nitrogen in the marine environment*, 2nd ed. Academic Press. doi:[10.1016/B978-0-12-372522-6.00001-3](https://doi.org/10.1016/B978-0-12-372522-6.00001-3)
- Harms, N. C., and others. 2019. Nutrient distribution and nitrogen and oxygen isotopic composition of nitrate in water masses of the subtropical southern Indian Ocean. *Biogeosciences* **16**: 2715–2732. doi:[10.5194/bg-16-2715-2019](https://doi.org/10.5194/bg-16-2715-2019)
- Hermes, J. C., and others. 2019. A sustained ocean observing system in the Indian Ocean for climate related scientific knowledge and societal needs. *Front. Mar. Sci.* **6**: 355. doi:[10.3389/fmars.2019.00355](https://doi.org/10.3389/fmars.2019.00355)
- Hood, R. R., J. D. Wiggert, and S. W. A. Naqvi. 2009. Indian Ocean research: Opportunities and challenges, p. 409–429. In J. D. Wiggert, R. R. Hood, S. W. A. Naqvi, K. H. Brink, and S. L. Smith [eds.], *Indian Ocean biogeochemical processes and ecological variability*. American Geophysical Union. doi:[10.1029/2007GM000714](https://doi.org/10.1029/2007GM000714)
- Hood, R. R., S. Wajih, A. Naqvi, J. D. Wiggert, and A. Subramaniam. 2007. Biogeochemical and ecological research in the Indian ocean. *Eos* **88**: 144. doi:[10.1029/2007eo120007](https://doi.org/10.1029/2007eo120007)
- Hood, R. R., and others. 2015. Science plan of the second international Indian Ocean expedition (IIOE-2): A basin-wide research program. (2015–2020). Report Scientific Committee on Oceanic Research.
- Hood, R. R., L. E. Beckley, and J. D. Wiggert. 2017. Biogeochemical and ecological impacts of boundary currents in the Indian Ocean. *Prog. Oceanogr.* **156**: 290–325. doi:[10.1016/j.pocean.2017.04.011](https://doi.org/10.1016/j.pocean.2017.04.011)
- Hörstmann, C., E. J. Raes, P. L. Buttigieg, C. Lo Monaco, U. John, and A. M. Waite. 2021. Hydrographic fronts shape productivity, nitrogen fixation, and microbial community composition in the southern Indian Ocean and the Southern Ocean. *Biogeosciences* **18**: 3733–3749. doi:[10.5194/bg-18-3733-2021](https://doi.org/10.5194/bg-18-3733-2021)
- Jayakumar, A., and B. B. Ward. 2020. Diversity and distribution of nitrogen fixation genes in the oxygen minimum zones of the world oceans. *Biogeosciences* **17**: 5953–5966. doi:[10.5194/bg-17-5953-2020](https://doi.org/10.5194/bg-17-5953-2020)
- Jayakumar, A., M. M. D. Al-Rshaidat, B. B. Ward, and M. R. Mulholland. 2012. Diversity, distribution, and expression of diazotroph *nifH* genes in oxygen-deficient waters of the Arabian Sea. *FEMS Microbiol. Ecol.* **82**: 597–606. doi:[10.1111/j.1574-6941.2012.01430.x](https://doi.org/10.1111/j.1574-6941.2012.01430.x)
- Jayakumar, A., B. X. Chang, B. Widner, P. Bernhardt, M. R. Mulholland, and B. B. Ward. 2017. Biological nitrogen fixation in the oxygen-minimum region of the eastern tropical North Pacific Ocean. *ISME J.* **11**: 2356–2367. doi:[10.1038/ismej.2017.97](https://doi.org/10.1038/ismej.2017.97)
- Jiang, S., F. Hashihama, Y. Masumoto, H. Liu, H. Ogawa, and H. Saito. 2022. Phytoplankton dynamics as a response to physical events in the oligotrophic eastern Indian Ocean. *Prog. Oceanogr.* **203**: 102784. doi:[10.1016/j.pocean.2022.102784](https://doi.org/10.1016/j.pocean.2022.102784)
- Jinadasa, S. U. P., G. Pathirana, P. N. Ranasinghe, L. Centurioni, and V. Hormann. 2020. Monsoonal impact on circulation pathways in the Indian Ocean. *Acta Oceanol. Sin.* **39**: 103–112. doi:[10.1007/s13131-020-1557-5](https://doi.org/10.1007/s13131-020-1557-5)
- Jyothibabu, R., C. Karnan, L. Jagadeesan, N. Arunpandi, R. S. Pandiarajan, K. R. Muraleedharan, and K. K. Balachandran. 2017. *Trichodesmium* blooms and warm-core ocean surface features in the Arabian Sea and the Bay of Bengal. *Mar. Pollut. Bull.* **121**: 201–215. doi:[10.1016/j.marpolbul.2017.06.002](https://doi.org/10.1016/j.marpolbul.2017.06.002)
- Knapp, A. N., K. L. Casciotti, W. M. Berelson, M. G. Prokopenko, and D. G. Capone. 2016. Low rates of nitrogen fixation in eastern tropical South Pacific surface waters. *Proc. Natl. Acad. Sci. USA* **113**: 4398–4403. doi:[10.1073/pnas.1515641113](https://doi.org/10.1073/pnas.1515641113)
- Koné, V., O. Aumont, M. Lévy, and L. Resplandy. 2009. Physical and biogeochemical controls of the phytoplankton seasonal cycle in the Indian Ocean: A modeling study, p. 147–166. In J. D. Wiggert, R. R. Hood, S. W. A. Naqvi, K. H. Brink, and S. L. Smith [eds.], *Indian Ocean biogeochemical processes and ecological variability*. American Geophysical Union. doi:[10.1029/2008GM000700](https://doi.org/10.1029/2008GM000700)
- Kromkamp, J., M. De Bie, N. Goosen, J. Peene, P. Van Rijswijk, J. Sinke, and G. C. A. Duinevel. 1997. Primary production by phytoplankton along the Kenyan coast during the SE monsoon and November intermonsoon 1992, and the

- occurrence of *Trichodesmium*. Deep-Sea Res. II: Top. Stud. Oceanogr. **44**: 1195–1212. doi:[10.1016/S0967-0645\(97\)00015-5](https://doi.org/10.1016/S0967-0645(97)00015-5)
- Kumar, P. K., A. Singh, R. Ramesh, and T. Nallathambi. 2017. N₂ fixation in the eastern Arabian Sea: Probable role of heterotrophic diazotrophs. Front. Mar. Sci. **4**: 80. doi:[10.3389/fmars.2017.00080](https://doi.org/10.3389/fmars.2017.00080)
- Lachkar, Z., M. Lévy, and K. S. Smith. 2019. Strong intensification of the Arabian Sea oxygen minimum zone in response to Arabian gulf warming. Geophys. Res. Lett. **46**: 5420–5429. doi:[10.1029/2018GL081631](https://doi.org/10.1029/2018GL081631)
- Landolfi, A., A. E. F. Prowe, M. Pahlow, C. J. Somes, C.-T. Chien, M. Schartau, W. Koeve, and A. Oschlies. 2021. Can top-down controls expand the ecological niche of marine N₂ fixers? Front. Microbiol. **12**: 690200. doi:[10.3389/fmicb.2021.690200](https://doi.org/10.3389/fmicb.2021.690200)
- Li, L., C. Wu, D. Huang, C. Ding, Y. Wei, and J. Sun. 2021. Integrating stochastic and deterministic process in the biogeography of N₂-fixing cyanobacterium *Candidatus Atelocyanobacterium Thalassa*. Front. Microbiol. **12**: 654646. doi:[10.3389/fmicb.2021.654646](https://doi.org/10.3389/fmicb.2021.654646)
- Loescher, C. R., and others. 2014. Facets of diazotrophy in the oxygen minimum zone waters off Peru. ISME J. **8**: 2180–2192. doi:[10.1038/ismej.2014.71](https://doi.org/10.1038/ismej.2014.71)
- Löscher, C. R., W. Mohr, H. W. Bange, and D. E. Canfield. 2020. No nitrogen fixation in the Bay of Bengal? Biogeosciences **17**: 851–864. doi:[10.5194/bg-17-851-2020](https://doi.org/10.5194/bg-17-851-2020)
- Löscher, C. R., W. Mohr, H. W. Bange, and D. E. Canfield. 2020. No N₂ fixation in the Bay of Bengal? Biogeosciences **17**: 851–864. doi:[10.5194/bg-2019-347](https://doi.org/10.5194/bg-2019-347)
- Luo, Y.-W., and others. 2012. Database of diazotrophs in global ocean: Abundance, biomass and nitrogen fixation rates. Earth Syst. Sci. Data **4**: 47–73. doi:[10.5194/essd-4-47-2012](https://doi.org/10.5194/essd-4-47-2012)
- Madhupratap, M., S. P. Kumar, P. M. A. Bhattathiri, M. D. Kumar, S. Raghukumar, K. K. C. Nair, and N. Ramaiah. 1996. Mechanism of the biological response to winter cooling in the northeastern Arabian Sea. Nature **384**: 549–552. doi:[10.1038/384549a0](https://doi.org/10.1038/384549a0)
- Marshall, N. B. 1960. The Galathea expedition. Nature **187**: 443–444. doi:[10.1038/187443a0](https://doi.org/10.1038/187443a0)
- Martin, J. H., S. E. Fitzwater, and R. M. Gordon. 1990. Iron deficiency limits phytoplankton growth in Antarctic waters. Glob. Biogeochem. Cycles **4**: 5–12. doi:[10.1029/GB004i001p00005](https://doi.org/10.1029/GB004i001p00005)
- Mazard, S. L., N. J. Fuller, K. M. Orcutt, O. Bridle, and D. J. Scanlan. 2004. PCR analysis of the distribution of unicellular cyanobacterial diazotrophs in the Arabian Sea. Appl. Environ. Microbiol. **70**: 7355–7364. doi:[10.1128/AEM.70.12.7355-7364.2004](https://doi.org/10.1128/AEM.70.12.7355-7364.2004)
- McGowan, H., and A. Clark. 2008. Identification of dust transport pathways from Lake Eyre, Australia using Hysplit. Atmos. Environ. **42**: 6915–6925. doi:[10.1016/j.atmosenv.2008.05.053](https://doi.org/10.1016/j.atmosenv.2008.05.053)
- Measures, C. I., and S. Vink. 1999. Seasonal variations in the distribution of Fe and Al in the surface waters of the Arabian Sea. Deep-Sea Res. II: Top. Stud. Oceanogr. **46**: 1597–1622. doi:[10.1016/S0967-0645\(99\)00037-5](https://doi.org/10.1016/S0967-0645(99)00037-5)
- Metzl, N., C. Lo Monaco, C. Leseurre, C. Ridame, J. Fin, C. Mignon, M. Gehlen, and T. T. T. Chau. 2022. The impact of the South-East Madagascar Bloom on the oceanic CO₂ sink. Biogeosciences **19**: 1451–1468. doi:[10.5194/bg-19-1451-2022](https://doi.org/10.5194/bg-19-1451-2022)
- Michaels, A. F., and others. 1996. Inputs, losses and transformations of nitrogen and phosphorus in the pelagic North Atlantic Ocean. Biogeochemistry **35**: 181–226. doi:[10.1007/BF02179827](https://doi.org/10.1007/BF02179827)
- Mills, M. M., K. A. Turk-Kubo, G. L. van Dijken, B. A. Henke, K. Harding, S. T. Wilson, K. R. Arrigo, and J. P. Zehr. 2020. Unusual marine cyanobacteria/haptophyte symbiosis relies on N₂ fixation even in N-rich environments. ISME J.: 2395–2406. doi:[10.1038/s41396-020-0691-6](https://doi.org/10.1038/s41396-020-0691-6)
- Moffett, J. W., J. Vedamati, T. J. Goepfert, A. Pratihary, M. Gauns, and S. W. A. Naqvi. 2015. Biogeochemistry of iron in the Arabian Sea. Limnol. Oceanogr. **60**: 1671–1688. doi:[10.1002/lno.10132](https://doi.org/10.1002/lno.10132)
- Mulholland, M. R., and D. G. Capone. 2009. Dinitrogen fixation in the Indian Ocean, p. 167–186. In J. D. Wiggert, R. R. Hood, S. W. A. Naqvi, K. H. Brink, and S. L. Smith [eds.], *Indian Ocean biogeochemical processes and ecological variability*. American Geophysical Union. doi:[10.1029/2009GM000850](https://doi.org/10.1029/2009GM000850)
- Murtugudde, R. G., S. R. Signorini, J. R. Christian, A. J. Busalacchi, C. R. McClain, and J. Picaut. 1999. Ocean color variability of the tropical indo-Pacific basin observed by SeaWiFS during 1997–1998. J. Geophys. Res.: Oceans **104**: 18351–18366. doi:[10.1029/1999JC900135](https://doi.org/10.1029/1999JC900135)
- Naqvi, S. W. A. 1987. Some aspects of the oxygen-deficient conditions and denitrification in the Arabian Sea. J. Mar. Res. **45**: 1049–1072. doi:[10.1357/002224087788327118](https://doi.org/10.1357/002224087788327118)
- Naqvi, S. W. A., M. Voss, and J. P. Montoya. 2008. Recent advances in the biogeochemistry of nitrogen in the ocean. Biogeosci. Discuss. **5**: 1119–1137. doi:[10.5194/bg-5-1033-2008](https://doi.org/10.5194/bg-5-1033-2008)
- Naqvi, S. W. A., and others. 2009. Seasonal anoxia over the Western Indian continental shelf, p. 333–345. In J. D. Wiggert, R. R. Hood, S. W. A. Naqvi, K. H. Brink, and S. L. Smith [eds.], *Indian Ocean biogeochemical processes and ecological variability*. American Geophysical Union (AGU). doi:[10.1029/2008GM000745](https://doi.org/10.1029/2008GM000745)
- Parambil, A. V. 2015. Remote sensing and numerical modeling of the oceanic mixed layer salinity in the Bay of Bengal. Ph.D. thesis. Université Paul Sabatier.
- Phillips, H. E., and others. 2021. Progress in understanding of Indian Ocean circulation, variability, air–sea exchange, and impacts on biogeochemistry. Ocean Sci. **17**: 1677–1751. doi:[10.5194/os-17-1677-2021](https://doi.org/10.5194/os-17-1677-2021)
- Pierella Karlusich, J. J., and others. 2021. Global distribution patterns of marine nitrogen-fixers by imaging and

- molecular methods. *Nat. Commun.* **12**: 4160. doi:[10.1038/s41467-021-24299-y](https://doi.org/10.1038/s41467-021-24299-y)
- Postgate, J. R. 1982. Biology nitrogen fixation: Fundamentals. *Philos. Trans. R. Soc. B: Biol. Sci.* **296**: 375–385. doi:[10.1098/rstb.1982.0013](https://doi.org/10.1098/rstb.1982.0013)
- Poulton, A. J., M. C. Stinchcombe, and G. D. Quartly. 2009. High numbers of *Trichodesmium* and diazotrophic diatoms in the Southwest Indian Ocean. *Geophys. Res. Lett.* **36**. doi:[10.1029/2009GL039719](https://doi.org/10.1029/2009GL039719)
- Qin, W., and others. 2014. Marine ammonia-oxidizing archaeal isolates display obligate mixotrophy and wide ecotypic variation. *Proc. Natl. Acad. Sci. USA* **111**: 12504–12509. doi:[10.1073/pnas.1324115111](https://doi.org/10.1073/pnas.1324115111)
- Raes, E., A. Waite, A. McInnes, H. Olsen, H. Nguyen, N. Hardman-Mountford, and P. Thompson. 2014. Changes in latitude and dominant diazotrophic community alter N₂ fixation. *Mar. Ecol. Prog. Ser.* **516**: 85–102. doi:[10.3354/meps11009](https://doi.org/10.3354/meps11009)
- Raes, E. J., P. A. Thompson, A. S. McInnes, H. M. Nguyen, N. Hardman-Mountford, and A. M. Waite. 2015. Sources of new nitrogen in the Indian Ocean. *Glob. Biogeochem. Cycles* **29**: 1283–1297. doi:[10.1002/2015GB005194](https://doi.org/10.1002/2015GB005194)
- Raes, E. J., L. Bodrossy, J. van de Kamp, A. Bissett, and A. M. Waite. 2018. Marine bacterial richness increases towards higher latitudes in the eastern Indian Ocean. *Limnol. Oceanogr.* **3**: 10–19. doi:[10.1002/lol2.10058](https://doi.org/10.1002/lol2.10058)
- Resplandy, L., J. Vialard, M. Lévy, O. Aumont, and Y. Dandonneau. 2009. Seasonal and intraseasonal biogeochemical variability in the thermocline ridge of the southern tropical Indian Ocean. *J. Geophys. Res.: Oceans* **114**. doi:[10.1029/2008JC005246](https://doi.org/10.1029/2008JC005246)
- Roxy, M. K., and others. 2016. A reduction in marine primary productivity driven by rapid warming over the tropical Indian Ocean. *Geophys. Res. Lett.* **43**: 826–833. doi:[10.1002/2015GL066979](https://doi.org/10.1002/2015GL066979)
- Sarma, V. V. S. S., R. Vivek, D. N. Rao, and V. R. D. Ghosh. 2020. Severe phosphate limitation on nitrogen fixation in the Bay of Bengal. *Cont. Shelf Res.* **205**: 104199. doi:[10.1016/j.csr.2020.104199](https://doi.org/10.1016/j.csr.2020.104199)
- Sato, T., T. Shiozaki, F. Hashihama, M. Sato, A. Murata, K. Sasaoka, S. Umeda, and K. Takahashi. 2022. Low nitrogen fixation related to shallow Nitracline across the eastern Indian Ocean. *J. Geophys. Res.: Biogeosciences* **127**: e2022JG007104. doi:[10.1029/2022JG007104](https://doi.org/10.1029/2022JG007104)
- Saxena, H., D. Sahoo, M. A. Khan, S. Kumar, A. K. Sudheer, and A. Singh. 2020. Dinitrogen fixation rates in the Bay of Bengal during summer monsoon. *Environ. Res. Commun.* **2**: 051007. doi:[10.1088/2515-7620/ab89fa](https://doi.org/10.1088/2515-7620/ab89fa)
- Schott, F. A., and J. P. McCreary. 2001. The monsoon circulation of the Indian Ocean. *Prog. Oceanogr.* **51**: 1–123. doi:[10.1016/S0079-6611\(01\)00083-0](https://doi.org/10.1016/S0079-6611(01)00083-0)
- Schott, F. A., S.-P. Xie, and J. P. McCreary. 2009. Indian Ocean circulation and climate variability. *Rev. Geophys.* **47**. doi:[10.1029/2007RG000245](https://doi.org/10.1029/2007RG000245)
- Selden, C. R., M. R. Mulholland, P. W. Bernhardt, B. Widner, A. Macías-Tapia, Q. Ji, and A. Jayakumar. 2019. Dinitrogen fixation across physico-chemical gradients of the eastern tropical North Pacific oxygen deficient zone. *Glob. Biogeochem. Cycles* **33**: 1187–1202. doi:[10.1029/2019GB006242](https://doi.org/10.1029/2019GB006242)
- Selden, C. R., M. R. Mulholland, B. Widner, P. Bernhardt, and A. Jayakumar. 2021. Toward resolving disparate accounts of the extent and magnitude of nitrogen fixation in the Eastern Tropical South Pacific oxygen deficient zone. *Limnol. Oceanogr.* doi:[10.1002/lno.11735](https://doi.org/10.1002/lno.11735)
- Sewell, R. B. S. 1934. The John Murray expedition to the Arabian Sea. *Nature* **133**: 669–672. doi:[10.1038/133669a0](https://doi.org/10.1038/133669a0)
- Shao, Z., and Y. W. Luo. 2022. Controlling factors on the global distribution of a representative marine non-cyanobacterial diazotroph phylotype (Gamma A). *Biogeosciences* **19**: 2939–2952. doi:[10.5194/bg-19-2939-2022](https://doi.org/10.5194/bg-19-2939-2022)
- Shiozaki, T., M. Ijichi, T. Kodama, S. Takeda, and K. Furuya. 2014. Heterotrophic bacteria as major nitrogen fixers in the euphotic zone of the Indian Ocean: Nitrogen fixation in the Indian Ocean. *Glob. Biogeochem. Cycles* **28**: 1096–1110. doi:[10.1002/2014GB004886](https://doi.org/10.1002/2014GB004886)
- Singh, A., and R. Ramesh. 2011. Contribution of riverine dissolved inorganic nitrogen flux to new production in the coastal northern Indian Ocean: An assessment. *Int. J. Oceanogr.* **2011**: 983561. doi:[10.1155/2011/983561](https://doi.org/10.1155/2011/983561)
- Singh, A., and R. Ramesh. 2015. Environmental controls on new and primary production in the northern Indian Ocean. *Prog. Oceanogr.* **131**: 138–145. doi:[10.1016/j.pocean.2014.12.006](https://doi.org/10.1016/j.pocean.2014.12.006)
- Singh, A., N. Gandhi, and R. Ramesh. 2019. Surplus supply of bioavailable nitrogen through N₂ fixation to primary producers in the eastern Arabian Sea during autumn. *Cont. Shelf Res.* **181**: 103–110. doi:[10.1016/j.csr.2019.05.012](https://doi.org/10.1016/j.csr.2019.05.012)
- Smith, S. L. 2005. The Arabian Sea of the 1990s: New biogeochemical understanding. *Prog. Oceanogr.* **65**: 113–115. doi:[10.1016/j.pocean.2005.03.001](https://doi.org/10.1016/j.pocean.2005.03.001)
- Swallow, J. C. 1980. The Indian Ocean experiment: Introduction. *Science* **209**: 588. doi:[10.1126/science.209.4456.588.a](https://doi.org/10.1126/science.209.4456.588.a)
- Swallow, J. C. 1984. Some aspects of the physical oceanography of the Indian Ocean. *Deep-Sea Res. A: Oceanogr. Res. Pap.* **31**: 639–650. doi:[10.1016/0198-0149\(84\)90032-3](https://doi.org/10.1016/0198-0149(84)90032-3)
- Tang, W., Z. Li, and N. Cassar. 2019a. Machine learning estimates of global marine nitrogen fixation. *J. Geophys. Res.: Biogeosciences* **124**: 717–730. doi:[10.1029/2018JG004828](https://doi.org/10.1029/2018JG004828)
- Tang, W., S. Wang, D. Fonseca-Batista, and others. 2019b. Revisiting the distribution of oceanic N₂ fixation and estimating diazotrophic contribution to marine production. *Nat. Commun.* **10**: 1–10. doi:[10.1038/s41467-019-08640-0](https://doi.org/10.1038/s41467-019-08640-0)
- Terray, P., S. Dominiak, and P. Delécluse. 2005. Role of the southern Indian Ocean in the transitions of the monsoon-ENSO system during recent decades. *Clim. Dyn.* **24**: 169–195. doi:[10.1007/s00382-004-0480-3](https://doi.org/10.1007/s00382-004-0480-3)

- Thandlam, V., T. V. S. Udaya Bhaskar, R. Hasibur, P. D. Luca, E. Sahlée, A. Rutgersson, M. Ravichandran, and S. S. V. V. Ramakrishna. 2020. A sea-level monopole in the equatorial Indian Ocean. *npj Clim. Atmos. Sci.* **3**: 25. doi:[10.1038/s41612-020-0127-z](https://doi.org/10.1038/s41612-020-0127-z)
- Thi Dieu Vu, H., and Y. Sohrin. 2013. Diverse stoichiometry of dissolved trace metals in the Indian Ocean. *Sci. Rep.* **3**: 1745. doi:[10.1038/srep01745](https://doi.org/10.1038/srep01745)
- Turk-Kubo, K., K. Achilles, T. Serros, M. Ochiai, J. Montoya, and J. Zehr. 2012. Nitrogenase (*nifH*) gene expression in diazotrophic cyanobacteria in the tropical North Atlantic in response to nutrient amendments. *Front. Microbiol.* **3**: 386. doi:[10.3389/fmicb.2012.00386](https://doi.org/10.3389/fmicb.2012.00386)
- Turk-Kubo, K. A., M. R. Gradoville, S. Cheung, F. M. Cornejo-Castillo, K. J. Harding, M. Morando, M. Mills, and J. P. Zehr. 2022. Non-cyanobacterial diazotrophs: Global diversity, distribution, ecophysiology, and activity in marine waters. *FEMS Microbiol. Rev.* doi:[10.1093/femsre/fuac046](https://doi.org/10.1093/femsre/fuac046)
- Venables, H., and C. M. Moore. 2010. Phytoplankton and light limitation in the Southern Ocean: Learning from high-nutrient, high-chlorophyll areas. *J. Geophys. Res.* **115**. doi:[10.1029/2009jc005361](https://doi.org/10.1029/2009jc005361)
- Vinayachandran, P. N., P. A. Francis, and S. A. Rao. 2009. Indian Ocean dipole: Processes and impacts. *Curr. Trends Sci.* **46**: 569–589.
- Vinayachandran, P. N. M., and others. 2021. Reviews and syntheses: Physical and biogeochemical processes associated with upwelling in the Indian Ocean. *Biogeosciences* **18**: 5967–6029. doi:[10.5194/bg-18-5967-2021](https://doi.org/10.5194/bg-18-5967-2021)
- Wang, W.-L., J. K. Moore, A. C. Martiny, and F. W. Primeau. 2019. Convergent estimates of marine nitrogen fixation. *Nature* **566**: 205–211. doi:[10.1038/s41586-019-0911-2](https://doi.org/10.1038/s41586-019-0911-2)
- Wang, Y., and others. 2021. Metagenomic analysis reveals microbial community structure and metabolic potential for nitrogen acquisition in the oligotrophic surface water of the Indian Ocean. *Front. Microbiol.* **12**: 518865. doi:[10.3389/fmicb.2021.518865](https://doi.org/10.3389/fmicb.2021.518865)
- Ward, B. B., A. H. Devol, J. J. Rich, B. X. Chang, S. E. Bulow, H. Naik, A. Pratihary, and A. Jayakumar. 2009. Denitrification as the dominant nitrogen loss process in the Arabian Sea. *Nature* **461**: 78–81. doi:[10.1038/nature08276](https://doi.org/10.1038/nature08276)
- Weiss, R. F. 1983. *GEOSECS Indian Ocean Expedition: Hydrographic data 1977-1978*.
- Wiggert, J. D., R. G. Murtugudde, and J. R. Christian. 2006. Annual ecosystem variability in the tropical Indian Ocean: Results of a coupled bio-physical ocean general circulation model. *Deep-Sea Res. II: Top. Stud. Oceanogr.* **53**: 644–676. doi:[10.1016/j.dsr2.2006.01.027](https://doi.org/10.1016/j.dsr2.2006.01.027)
- Wiggert, J. D., and R. G. Murtugudde. 2007. The sensitivity of the southwest monsoon phytoplankton bloom to variations in aeolian iron deposition over the Arabian Sea. *J. Geophys. Res.: Oceans* **112**. doi:[10.1029/2006JC003514](https://doi.org/10.1029/2006JC003514)
- Wiggert, J. D., J. Vialard, and M. J. Behrenfeld. 2009. Basin-wide modification of dynamical and biogeochemical processes by the positive phase of the Indian Ocean dipole during the SeaWiFS era, p. 385–407. In J. D. Wiggert, R. R. Hood, S. W. A. Naqvi, K. H. Brink, and S. L. Smith [eds.], *Indian Ocean biogeochemical processes and ecological variability*. American Geophysical Union (AGU). doi:[10.1029/2008GM000776](https://doi.org/10.1029/2008GM000776)
- Wu, C., J. Kan, H. Liu, L. Pujari, C. Guo, X. Wang, and J. Sun. 2019. Heterotrophic bacteria dominate the diazotrophic community in the Eastern Indian Ocean (EqIO) during pre-southwest monsoon. *Microb. Ecol.* **78**: 804–819. doi:[10.1007/s00248-019-01355-1](https://doi.org/10.1007/s00248-019-01355-1)
- Wu, C., J. Sun, H. Liu, W. Xu, G. Zhang, H. Lu, and Y. Guo. 2021. Evidence of the significant contribution of heterotrophic diazotrophs to nitrogen fixation in the eastern Indian Ocean during pre-southwest monsoon period. *Ecosystems* **25**: 1066–1083. doi:[10.1007/s10021-021-00702-z](https://doi.org/10.1007/s10021-021-00702-z)
- Wu, C., D. D. Narale, Z. Cui, X. Wang, H. Liu, W. Xu, G. Zhang, and J. Sun. 2022. Diversity, structure, and distribution of bacterioplankton and diazotroph communities in the Bay of Bengal during the winter monsoon. *Front. Microbiol.* **13**: 987462. doi:[10.3389/fmicb.2022.987462](https://doi.org/10.3389/fmicb.2022.987462)
- Wyrtki, K., E. B. Bennett, and D. J. Rochford. 1971. *Oceanographic atlas of the international Indian Ocean expedition*, v. **531**. National Science Foundation.
- Zehr, J. P., and B. B. Ward. 2002. Nitrogen cycling in the ocean: New perspectives on processes and paradigms. *Appl. Environ. Microbiol.* **68**: 1015–1024. doi:[10.1128/AEM.68.3.1015-1024.2002](https://doi.org/10.1128/AEM.68.3.1015-1024.2002)
- Zehr, J. P., B. D. Jenkins, S. M. Short, and G. F. Steward. 2003. Nitrogenase gene diversity and microbial community structure: A cross-system comparison. *Environ. Microbiol.* **5**: 539–554. doi:[10.1046/j.1462-2920.2003.00451.x](https://doi.org/10.1046/j.1462-2920.2003.00451.x)
- Zehr, J. P., and D. G. Capone. 2020. Changing perspectives in marine nitrogen fixation. *Science* **368**: eaay9514. doi:[10.1126/science.aay9514](https://doi.org/10.1126/science.aay9514)

Acknowledgments

This work was funded by the project DINDE granted to MB and AS by the Indo-French Centre for the Promotion of Advanced Research (IFCPAR/CEIPRA). DINDE is endorsed by the International Indian Ocean Expedition II under project endorsement number IIOE2-EP41. This work is also funded by project IDEFIX granted by the Pure Ocean Fund to MB. Part of the data compiled were obtained thanks to the OISO program cruise OISO-30 (<https://doi.org/10.17600/18000679>) supported by the French institutes INSU (Institut National des Sciences de l'Univers) and IPEV (Institut Polaire Paul-Emile Victor), OSU Ecce-Terra (at Sorbonne Université), and the French program SOERE/Great-Gases. The authors are indebted to Christian Furbo Reeder for his assistance with illustrations. SC was supported by a Campus France scholarship funded by IFCPAR/CEIPRA.

Submitted 14 December 2022

Revised 12 June 2023

Accepted 27 June 2023